

T cell–induced CSF1 promotes melanoma resistance to PD1 blockade

Natalie J. Neubert, Martina Schmittnaegel, Natacha Bordry, Sina Nassiri, Noémie Wald, Christophe Martignier, Laure Tillé, Krisztian Homicsko, William Damsky, Hélène Maby-El Hajjami, Irina Klamann, Esther Danenberg, Kalliopi Ioannidou, Lana Kandalaf, George Coukos, Sabine Hoves, Carola H. Ries, Silvia A. Fuertes Marraco, Periklis G. Foukas, Michele De Palma and Daniel E. Speiser

Sci Transl Med **10**, eaan3311.
DOI: 10.1126/scitranslmed.aan3311

CSF1 curbs immunotherapy efficacy in melanoma

Although melanoma is one of the cancer types best targeted by checkpoint blockade, many patients are refractory to therapy. One likely culprit is the persistence of tumor-associated macrophages, which can be immunosuppressive. Neubert and colleagues examined patient samples and performed coculture experiments that implicated CD8⁺ T cell induction of tumor-derived CSF1, which could then promote immunosuppressive macrophages. Addition of CSF1 signaling blockade to anti-PD1 treatment improved responses in transplantable mouse melanoma models. These results uncover the biology of hurdles that still need to be overcome in immunotherapy, and also suggest a solution.

ARTICLE TOOLS	http://stm.sciencemag.org/content/10/436/eaan3311
SUPPLEMENTARY MATERIALS	http://stm.sciencemag.org/content/suppl/2018/04/09/10.436.eaan3311.DC1
RELATED CONTENT	http://stm.sciencemag.org/content/scitransmed/9/407/eaal4712.full http://stm.sciencemag.org/content/scitransmed/9/379/eaah3560.full http://stm.sciencemag.org/content/scitransmed/9/389/eaal3604.full http://stm.sciencemag.org/content/scitransmed/9/392/eaal0225.full http://science.sciencemag.org/content/sci/359/6382/1350.full
REFERENCES	This article cites 106 articles, 39 of which you can access for free http://stm.sciencemag.org/content/10/436/eaan3311#BIBL
PERMISSIONS	http://www.sciencemag.org/help/reprints-and-permissions

Use of this article is subject to the [Terms of Service](#)

Supplementary Materials for

T cell–induced CSF1 promotes melanoma resistance to PD1 blockade

Natalie J. Neubert, Martina Schmittnaegel, Natacha Bordry, Sina Nassiri, Noémie Wald, Christophe Martignier, Laure Tillé, Krisztian Homicsko, William Damsky, Hélène Maby-El Hajjami, Irina Klamann, Esther Danenberg, Kalliopi Ioannidou, Lana Kandalaft, George Coukos, Sabine Hoves, Carola H. Ries, Silvia A. Fuertes Marraco, Periklis G. Foukas, Michele De Palma, * Daniel E. Speiser*

*Corresponding author. Email: michele.depalma@epfl.ch (M.D.P.); doc@dspeiser.ch (D.E.S.)

Published 11 April 2018, *Sci. Transl. Med.* **10**, eaan3311 (2018)
DOI: 10.1126/scitranslmed.aan3311

The PDF file includes:

Materials and Methods

Fig. S1. Selection of regions with high or low density of tumor-infiltrating CD8⁺ T cells.

Fig. S2. Correlations between genes expressed in the SKCM metastatic cohort.

Fig. S3. CSF1⁺ cell density in high and low CD8⁺ cell-infiltrated tumor regions.

Fig. S4. CSF1 expression by melanoma cell lines and CTLs.

Fig. S5. Absence of CSF1R on the surface of untreated or cytokine-treated melanoma cell lines.

Fig. S6. Gene expression in human melanoma cells exposed to MelanA-specific CTLs or IFN γ and TNF α .

Fig. S7. Expression of macrophage genes in a transcriptomic data set of human melanoma treated with anti-PD1 therapy.

Fig. S8. Impact of CTL and TAM infiltrates on melanoma prognosis.

Fig. S9. Concentration of CSF1 in cell culture medium conditioned by mouse melanoma cells.

Table S1. Melanoma patients, clinical parameters, and specimens analyzed in this study.

Table S2. Origin of the melanoma cell lines used in this study.

Table S3. List of melanoma-derived macrophage signature genes.

Table S4. A selection of currently active clinical trials of CSF1 or CSF1R blockade in combination with immune checkpoint blockade (ClinicalTrials.gov; 18 October 2017).

References (86–109)

Other Supplementary Material for this manuscript includes the following:
(available at
www.sciencetranslationalmedicine.org/cgi/content/full/10/436/eaan3311/DC1)

Table S5 (Microsoft Excel format). Primary raw data shown in the figures.

Materials and Methods

Collection of peripheral blood

Healthy volunteers and melanoma patients provided peripheral blood. For serum isolation, native blood was centrifuged for 15 min at $1200 \times g$. For plasma and peripheral blood mononuclear cell (PBMC) isolation, blood collected in tubes containing Li-heparin-coated beads (Sarstedt) was centrifuged for 10 min at $210 \times g$ to obtain plasma, followed by the preparation of PBMCs by gradient centrifugation using Lymphoprep (Ficoll equivalent; Axis-Shield). Cells were used either before or after cryopreservation. Viable cell recovery was consistently above 85%.

Human cell cultures

Melanoma cell lines were generated from metastases or tumor-infiltrated lymph node specimens from HLA-A2⁺ patients with histologically proven metastatic melanoma (**Table S2**) and were a kind donation from Donata Rimoldi (Ludwig Center for Cancer Research of the University of Lausanne). All melanoma cell lines had been cultured for less than six months after their generation at the time of the experiments (<P26). Melanoma cell lines used for CTL-melanoma cell co-cultures were MelanA/MART1-positive (confirmed by FACS). Autologous or HLA-matched MelanA/MART1-specific CD8⁺ T cell clones (CTLs) were isolated from melanoma patient blood and amplified by restimulation with PHA, irradiated feeder cells, and hrIL2 (86). All cell lines tested negative by mycoplasma-specific PCR before use and were authenticated using the PowerPlex 21 system (Promega) or PCR-SSO in November / December 2016, as described (49).

Melanoma cell lines were cultured in RPMI 1640/GlutaMAX-I, complemented with 10% heat-inactivated FCS (PAA), 1.1 μ M Arginine (Sigma Aldrich), 0.48 μ M Asparagine (Sigma Aldrich), 11.25 μ M Glutamine (Gibco), 10 mM Hepes (Gibco), and 100 U/ml of penicillin/streptomycin (Gibco). Where indicated, melanoma cell lines were cultured in the presence of IFN γ (222 U/ml; Peprotech), TNF α (50 ng/ml; Peprotech) or TNF α and IFN γ (10 ng/ml and 222 U/ml). The CTL-melanoma cell co-cultures were performed at a 1:1 ratio in medium supplemented with IL-2 (30 U/ml). Co-culture parameters, controls and setup were performed as described in (48) and in the figure legends. Transwell assays were performed in 12-well polyester transwell plates with 0.4 μ m pore size (Corning). For blocking experiments, we used TNF α (10 μ g/ml, clone 28401, R&D Systems) and IFN γ (10 μ g/ml, clone 25718, R&D Systems) blocking antibodies or isotype controls (clones 11711 and 20102, respectively).

Mouse cell cultures

The murine *BRAF*^{V600E} SM1-OVA melanoma cell line was kindly provided by Antoni Ribas (UCLA, US) (57, 87); the murine B16 cell line was kindly provided by Karine Breckpot (Vrije Universiteit Brussel, Brussels, Belgium); the murine Yummer1.7 cell line (58) was kindly provided by Marcus Bosenberg and Susan Kaech (Yale University, New Haven, CT, USA).

For CSF1 ELISA of B16, SM1-OVA or Yummer1.7 cell culture supernatants, 7×10^4 cells were seeded in

a 12-well plate (Costar) in 750 μ l of medium. B16 and SM1-OVA cells were cultured in RPMI 1640/GlutaMAX-I and Iscove's modified Dulbecco's medium (IMDM; Sigma) with 11.25 μ M glutamine (Gibco), respectively, both completed with 10% heat-inactivated fetal calf serum (FCS) and 100 U/ml of penicillin/streptomycin (Gibco). Yummer1.7 cells were cultured in DMEM/F12 medium (Gibco) with 10% FBS in L-glutamine (1%), Pen/Strep (1%), and MEM NEAA (1%, Gibco). After 24 and 48 hours in culture, the cell supernatant was collected and analyzed according to the manufacturer's instructions (see "ELISA" below).

Transplant tumor models

SM1-OVA melanoma cells (57) were expanded by injection of 1×10^6 cells into the right flank of NOD.Cg-*Prkdc^{scid} Il2rg^{tm1Wjl}/SzJ* (NSG) mice (Charles River). When tumors reached a size of 500-800 mm³, they were harvested and minced using a razor blade followed by digestion with collagenase IV (0.2 mg/ml, Worthington), dispase (2 mg/ml, Life Technologies) and DNase I (0.1 mg/ml, Life Technologies) in IMDM medium (without any supplements) for 30 min at 37°C. Cell suspensions were filtered using a cell strainer (70 μ m) and washed in PBS. Tumor cells were counted using trypan blue to determine viable cells, and 1×10^6 cells were injected into the right flank of C57BL/6N mice. Yummer1.7 tumors (58) were generated by injecting 0.5×10^6 Yummer1.7 cells subcutaneously in the right flank of C57BL/6N mice. C57BL/6N mice were purchased from Charles River Laboratory (L'Arbresle, France). All procedures were performed according to a protocol approved by the Veterinary Authorities of the Canton Vaud according to the Swiss Law (protocol 3049).

iBIP2 transgenic melanoma model

The iBIP2 mice were generated at EPFL in the laboratory of Prof. Douglas Hanahan based on the iBIP mice previously generated by the group of Linda Chin (59). The original iBIP mice harbor homozygous germ-line deletion of the *Cdkn2a* locus, floxed *Pten* alleles, and an inducible *Braf^{V600E}* allele. To generate iBIP2 mice, the *Cdkn2a* locus was modified to introduce homozygous floxed alleles of *Cdkn2a*. Therefore, in addition to floxed *Cdkn2a* alleles, iBIP2 mice harbor homozygous floxed alleles of *Pten* and three transgenes: TetO-*Braf^{V600E}*, tyrosinase-CreER^{T2}, and Rosa26-lsl-rtTA, which enable conditional *Cdkn2a* and *Pten* deletion and *Braf^{V600E}* expression specifically in the skin melanocytes. As a result, the iBIP2 model has a wild-type tumor microenvironment, in contrast to the iBIP model, in which cells of the tumor microenvironment are also genetically modified.

iBIP2 tumors were initiated at 6 weeks of age by topical application of 1 μ l of tamoxifen on the ear skin. Tumor initiation is sustained by the addition of doxycycline in the food pellets after initiation of the tumors by tamoxifen and throughout the experiment. iBIP2 mice were bred and maintained in the SPF unit of the EPFL animal facility. All procedures were performed according to a protocol approved by the Veterinary Authorities of the Canton Vaud according to the Swiss Law (protocol 3100).

Therapeutic trials in mouse melanoma models

Therapeutic monoclonal antibodies (mAbs) were obtained from Roche (Penzberg, Germany) or BioXCell

(<https://bxc.com>) and given at the following dosage regimens: rat anti-PD1 (clone RMPI-14; 10 mg/kg 3x/week) (88); rat anti-CSF1R (clone AFS98, used for transplant melanoma models; 50 mg/kg 3x/week) (72); mouse anti-CSF1R (clone 2G2, used for the iBIP2 transgenic melanoma model; 30 mg/kg, weekly) (31); control rat IgG2a (clone 2A3; 10 mg/kg or 50 mg/kg, 3x/week); control mouse IgG1 (MOPC; 30 mg/kg, weekly).

Treatment of mice carrying SM1-OVA or Yummer1.7 tumors started when the tumors reached a size of approximately 50 mm³ (day 4 to 7 post-injection). Treatment of iBIP2 mice started when the tumors reached a size of approximately 50-100 mm³. All mouse cohorts received mAb injections at the dosage regimens indicated above. In the Yummer1.7 experiment, mice received the last injection of therapeutic antibodies at day 27 after tumor challenge. Tumors were monitored several times *per* week and the mice euthanized when the tumors reached the termination volume of 1000 mm³.

Preparation of mouse tumors and spleens for flow cytometry

Tumors were harvested, minced and digested as described in the tumor model section above. Spleens were harvested and splenocytes obtained by mechanical disruption of the tissue in ice-cold IMDM (Sigma). Cell suspensions were filtered using a cell strainer (70 µm), washed in washing buffer (PBS containing 2 mM EDTA and 2% FBS), and red blood cells lysed using erythrocyte lysis buffer (Sigma) for 5 minutes at room temperature. About 1x10⁶ cells were diluted in 100 µl of washing buffer per FACS tube. All cell suspensions (see procedures below) were incubated with rat anti-mouse FcγIII/II receptor (CD16/CD32) blocking antibodies (4 µg/ml, “Fc-block”), stained with conjugated antibodies, washed and resuspended in DAPI-containing buffer to exclude non-viable cells from further analyses. All samples were analyzed using the flow cytometer BD Bioscience LSRII SORP. Compensation was performed using fluorescence-minus-one (FMO) controls.

Flow cytometry of mouse tumors and spleens

Cells were discriminated using the following combinations of cell markers after gating on single cells (discriminated by FSC-A and FSC-H) and excluding non-viable cells.

- CD4⁺ T cells: CD45⁺CD11b⁻NK1.1⁻Tcrb⁺CD4⁺;
- CD8⁺ T cells: CD45⁺CD11b⁻NK1.1⁻Tcrb⁺CD8⁺;
- TAMs: CD45⁺CD11b⁺ Ly6C⁻Ly6G⁻F4/80⁺
- M2-like TAMs: CD45⁺CD11b⁺ Ly6C⁻Ly6G⁻F4/80⁺ MRC1⁺CD11c^{-/low};
- Monocytes and mo-MDSCs: CD45⁺CD11b⁺Ly6C⁺Ly6G⁻
- Neutrophils and gr-MDSCs: CD45⁺CD11b⁺Ly6G⁺Ly6C⁻
- CD11b⁻ non-myeloid cells: CD45⁺CD11b⁻

All antibodies were obtained from eBioscience (anti-CD45: clone 30_F11; anti-Ly6C: clone HK1.4; anti-Ly6G: clone 1A8; anti-Tcrb: clone H57-597), Invitrogen (anti-CD8: clone 5H10) or BioLegend (anti-CD11b: clone M1/70; CD11c: clone N418; anti-MRC1: clone C068C2; anti-F4/80: clone BM8; anti-CD4: clone RM4-5; anti-NK1.1: clone PK136).

Flow cytometry of human melanoma cell lines

The following antibodies specific for human proteins were used: rat anti-CSF1R (PE, clone 12-3A3-1B10, eBioscience), polyclonal rabbit anti-CSF1 (Antigenix; labeled in-house with Alexa 647) and isotype control rat IgG2a kappa (PE, clone 12-4321-42, eBioscience). For protein expression analyses of melanoma cells after co-culture with CTLs, melanoma cells were analyzed with a Gallios flow cytometer (Beckman Coulter, 3-laser configuration) and the data processed as described previously (see Suppl. Fig. S3A in (48)). In brief, melanoma cells were labeled with CFSE and CTLs were labeled with violet tracker (both Cell-trace Cell-Proliferation kit, Molecular Probes) prior to co-culture. Besides excluding debris and doublets by forward and side scatter analysis, dead cells were excluded by Vivid Aqua staining (LIVE/DEAD Fixable Aqua Dead Cell Stain Kit, Life Technologies). CTLs and melanoma cells were separated based on their CFSE and violet tracker label. For cultures in absence of CTLs (treatment with IFN γ and TNF α), melanoma cells were not labeled prior to culture. For mRNA analysis of melanoma cells after co-culture with CTLs, melanoma cells were isolated from the co-culture using the Astrios sorter (Beckman Coulter), as described previously (see Suppl. Fig. S1A in (49)). Briefly, debris, doublets and the majority of CTLs were removed according to forward-sideward scatter properties. Dead cells were excluded by DAPI staining. Melanoma cells were identified by gating on the CFSE-positive, violet-tracker-negative population. Data were analyzed with FlowJo (Tree Star Inc., version 9.7) and Graphpad Prism (version 6).

ELISA

The CSF1 concentration in culture supernatant, serum samples and plasma samples was determined using the human or mouse CSF1 Quantikine ELISA kit (R&D Systems) according to the manufacturer's instructions. The IFN γ concentration was measured by ELISA with human IFN γ -specific antibodies from Invitrogen (capture antibody AHC4432; detection antibody AHC4539).

Quantification of CSF1 RNA in melanoma cell lines

mRNA was extracted from melanoma cells using the Pico Pure RNA isolation kit (Arcturus) according to the kit instructions, and CSF1 mRNA abundance was determined with the NanoString nCounter technology at the iGE3Genomics platform, University of Geneva. Normalized expression values were calculated as described previously (48). *RPLP0*, *GUSB*, *ALG12*, *ADAT2* and *KRBA2* gene transcripts were used for normalization.

qPCR analysis of mouse tumor samples

Small tissue fragments were obtained from tumors excluding the necrotic area. Freshly dissected pieces of tumor fragments were frozen on dry ice and stored at -80°C until further use. Total mRNA was purified following RNeasy Mini kit guidelines (Qiagen). RNA was quantified with a NanoDrop ND-2000 and retrotranscribed using SuperScript Vilo cDNA synthesis kit (Invitrogen), according to manufacturer's instructions. All qPCR reactions were performed using the following TaqMan gene assays: *Adgre1* (Mm00802529_m1), *Mrc1* (Mm01329362-m1), *Ifng* (Mm01168134_m1), *Csf1* (Mm00432686_m1), *Ccl2* (Mm00441242_m1), *Il4* (Mm00445259_m1), *Cxcl12*

(Mm00445553_m1), *Cxcl1* (Mm04207460_m1), *Csf2* (Mm01290062_m1), *Gapdh* (Mm99999915-g1), and *Hprt* (Mm02800695_m1), all from Applied Biosystems/Life Technologies. Each assay was performed in 3 technical replicates using 10 ng of total cDNA per reaction and TaqMAN Universal master mix (Life Technologies). qPCR was run for 40 cycles in standard mode using an ABI7900HT apparatus (Applied Biosystems). After qPCR, raw data were extracted and evaluated using the SDS software v2.4. For the analysis of the results, we calculated the average of the median threshold cycle (C_t) of 2 reference genes (*Hprt* and *Gapdh*) (C_t reference) for each sample triplicate. In order to normalize gene expression data among different samples, the C_t reference value is subtracted from the median C_t value (C_t gene) of the gene of interest (ΔC_t):

$$\Delta C_t = C_t \text{ gene of interest} - C_t \text{ reference}$$

The normalized expression value of the control sample (ΔC_t control; typically the IgG-treated sample) is then subtracted from the normalized expression value of the sample of interest ($\Delta \Delta C_t$):

$$\Delta \Delta C_t = \Delta C_t \text{ sample} - \Delta C_t \text{ control}$$

The expression level of the gene of interest (relative to the control sample) is given by the following equation:

$$\text{Expression level} = 2^{-\Delta \Delta C_t}$$

This equation is based on the assumption that the amplification efficiency is 2, meaning that the product DNA is doubled after each cycle during the exponential phase of the PCR reaction. Statistical analysis of gene expression data was performed on the fold-change values.

Chromogenic immunohistochemistry (IHC) staining and quantification

IHC was performed on consecutive 4- μ m paraffin sections from surgical specimens of primary melanomas and metastases from the patients listed in **Table S1**. The following primary antibodies were used: rabbit polyclonal anti-CSF1 (1:100, Antigenix America), mouse monoclonal anti-CSF1R (clone 29 pRED, 1:2800, Roche Penzberg), mouse monoclonal anti-CD8 (SP57, RTU, Ventana), and mouse monoclonal anti-CD163 (clone MRQ-26, RTU, Ventana). Slides were placed on a BenchMark XT slide stainer (Ventana; Roche) for deparaffinization, endogenous peroxidase quenching, and epitope retrieval. UltraView Universal DAB Detection Kit (Ventana) was used for anti-CD8 and OpticView DAB detection Kit (Ventana) was used for anti-CSF1, anti-CSF1R and anti-CD163 staining. All stains included a negative control with a matched antibody isotype, whereas staining of tonsillar, bladder and colorectal cancer sections served as positive controls for all antibodies.

Stained slides were scanned in a batch format by using the Vectra multispectral imaging system (Perkin-Elmer), and lower power field images of the entire tissue were first collected. Then, an average of 4 high power fields (HPF; 20x magnification) were chosen within tumor regions with either high or low infiltrating CD8⁺ cells (see Fig. S1). The same regions were selected for acquiring CSF1, CD163 and CSF1R immunostaining. The selected 20 \times HPF images were subsequently processed by using the inForm tissue finder software (PerkinElmer). For unmixing of the images and analysis, spectral libraries of hematoxylin and DAB were generated. For CSF1 and CD8 staining, the selected HPF images were first segmented using the counterstained-based cell segmentation algorithm, and the number of positive cells calculated through nuclei threshold analysis. For CSF1R and CD163 staining, the HPF images were segmented using the object-based cell segmentation algorithm, and the number of

positive cells calculated through nuclei threshold analysis. Thresholds used to determine the cutoff for all four antibody stainings were set visually and approved by a trained pathologist.

Multiplexed immunofluorescence staining and multispectral image analysis

Multiplexed immunofluorescence was performed on 4 μm formalin-fixed, paraffin-embedded sections from complete excisions of primary melanomas and metastases from the patients and specimens listed in **Table S1**. We used the automated Discovery ULTRA Staining Module (Ventana, Roche) and the Tyramide signal amplification (TSA) method. Staining was done in consecutive rounds and each round consisted of: antigen retrieval, blocking solution, primary antibody, secondary HRP-labeled antibody, TSA and antibodies denaturation, as described previously (89). The sections were first deparaffinized by successive baths of xylene and rehydrated in a gradient of ethanol, followed by the step of heat-induced antigen retrieval using the buffer Cell Conditioning 1 (CC1, Ventana) for 32 minutes at 100°C. The blocking step consisted in incubation with Protein block buffer (Dako). The primary antibodies were then incubated at room temperature for 60 minutes. The following primary antibodies were used: rabbit monoclonal antibody anti-CSF1 (1:100, clone EP1179Y, Abcam), rabbit monoclonal antibody anti-CD8 (1:1000, Clone SP16, ThermoFisher Scientific) and rabbit polyclonal anti-S100 antibody (1:800, Novocastra). The signal was revealed with an HRP-labeled antibody polyclonal goat anti-rabbit Immunoglobulins/HRP (P044801, Dako) that was added at room temperature for 32 minutes. TSA was performed with the following reagents: TSA Cyanine 3 (NEL744B001KT, PerkinElmer) for CSF1 staining, TSA Cyanine 5 (NEL745B001KT, PerkinElmer) for CD8 staining, and TSA Fluorescein (NEL741B001KT, PerkinElmer) for S100 staining, at room temperature for 8 minutes. The antibody denaturation was done with incubation in Cell Conditioning 1 buffer (CC1, Ventana) for 24 minutes at 100°C. Sections were counterstained with DAPI (Biolegend, 1:4000) and coverslipped with mounting medium (S3023, Dako fluorescence mounting medium). A tonsil section was stained in parallel as a positive control.

Stained slides were scanned in a batch format using the Vectra multispectral imaging system (PerkinElmer), and lower power field images (10x) of the entire tissue were collected first. Then, we selected an average of five HPF (20x) images for each section in the tumor region via the Phenochart software (PerkinElmer). The selected 20 \times images were subsequently acquired and analyzed using inForm (v2.2, PerkinElmer). To unmix the emission spectra of each fluorophore, we generated a multispectral library of FITC, Cy3 and DAPI, as well as a spectrum of auto-fluorescence of the tissue (unstained section). The selected HPF images were first cell-segmented using the counterstained-based cell segmentation algorithm based on the DAPI staining and then the numbers of positive cells calculated through nuclei threshold analysis. Thresholds used to determine the cutoff for S100 and CSF1 antibodies stainings were set visually. The data shown in Fig. 3 are from the melanoma samples (four primary melanomas and four melanoma metastases) in which melanoma cells expressed S100; the S100-negative samples were excluded from the analysis.

For the data shown in Fig. S3, high CD8⁺ cell-infiltrated regions and low CD8⁺ cell-infiltrated regions in tumor nests were annotated and identified for high-resolution multispectral acquisition, at 20x magnification. The images were segmented into specific tissue categories of tumor nests and other tissue, based on the S100-positive

expression, after manually drawing training regions on each image (an average of 5 high HPF images were taken per selected region of interest). Individual cells were segmented using the counterstained-based cell segmentation algorithm. Cells were phenotyped into three different classes according to the markers of interest as follows: CD8-positive cells, CSF1-positive cells and cells negative for these two markers. After batch processing for high CD8⁺ cell-infiltrated regions and for low CD8⁺ cell-infiltrated regions, the pixel values were converted into values per mm² using the formula: pixels*0.246x10⁻⁶ = mm².

Bioinformatics analysis

Tumor mRNA (RNA-Seq V2) and clinical data from the SKCM subset of TCGA (46) were obtained from the cBioPortal for Cancer Genomics on Dec 29, 2016 (90, 91). RNA-Seq data including N=369 metastatic tumors were obtained as RSEM-normalized counts and log transformed for downstream analyses. Where applicable, the ratio of gene expressions was calculated as the numeric difference between log-transformed values. Correlation between selected genes was assessed using Spearman correlation coefficient. The 92-gene melanoma-derived macrophage-specific transcriptional signature was obtained from Ref. (55). Gene set analysis of the 91 genes present in the SKCM RNA-Seq data (46) was performed using the QuSAGE package from Bioconductor (92). Briefly, given a matrix of gene expression values, QuSAGE quantifies differential expression of a given gene set, while accounting for gene-gene correlations. Kaplan-Meier estimation of survival and log-rank test were performed using the survival package in R (93, 94). The long-rank p-values were adjusted for tumor stage. All bioinformatics analyses were performed in R (95).

FPKM-normalized gene expression data of response to anti-PD1 therapy in metastatic melanoma were downloaded from the Gene Expression Omnibus under accession number GSE78220 (56) and log transformed for downstream analyses.

Supplementary Figures

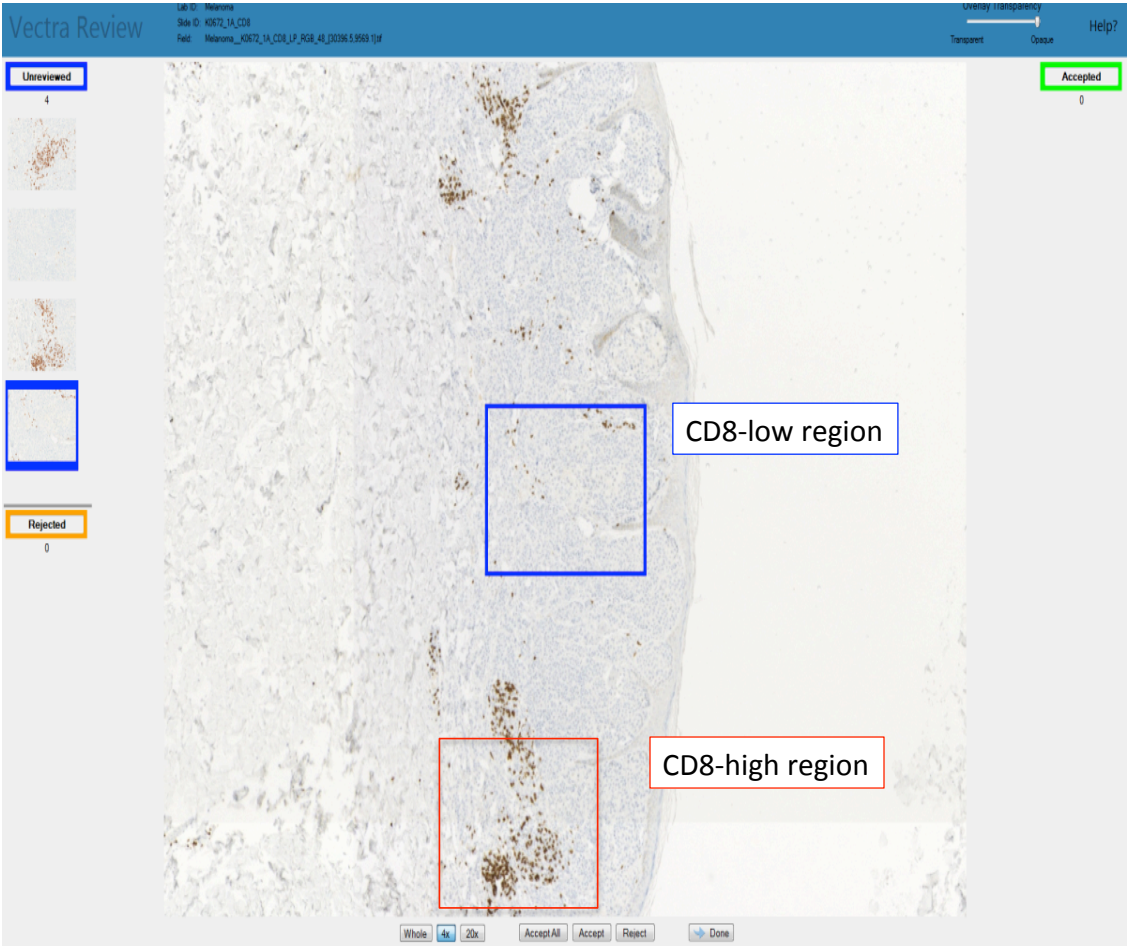


Fig. S1. Selection of regions with high or low density of tumor-infiltrating CD8⁺ T cells.
Examples of melanoma regions with either high or low CD8⁺ T cell density. Regions were selected using the Vectra system (Perkin Elmer), of which a snapshot is shown.

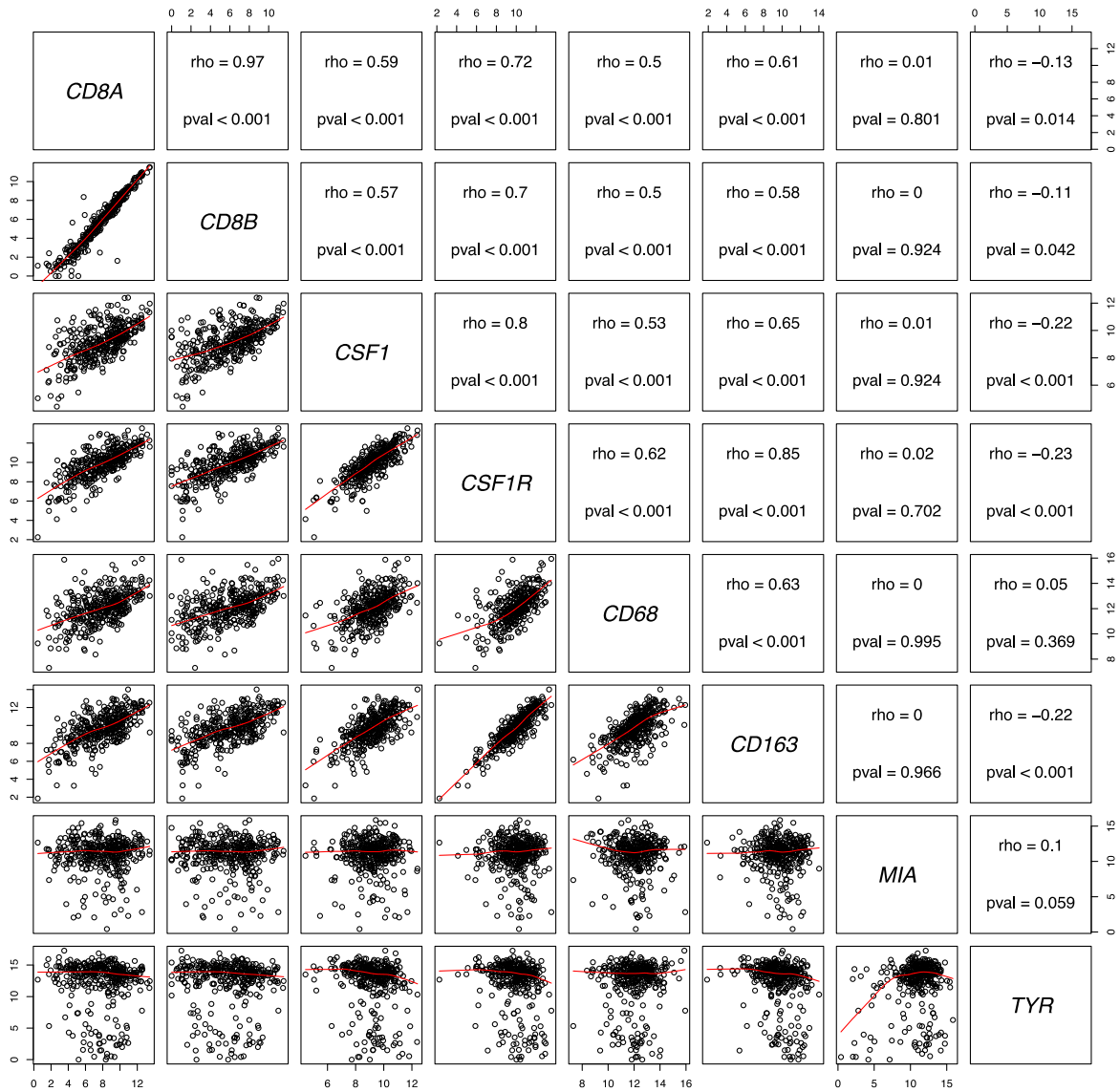


Fig. S2. Correlations between genes expressed in the SKCM metastatic cohort.

Extended matrix of scatterplots showing correlations between mRNA expression of *CD8A*, *CD8B*, *CSF1*, *CSF1R*, *CD68*, *CD163*, and melanoma-specific genes *MIA* and *TYR* as controls, in the SKCM metastatic cohort (N=369) of TCGA (46). Correlation was assessed using the Spearman correlation coefficient. Red lines indicate the local regression (LOESS) fit.

pval, P value; rho, Spearman's correlation coefficient.

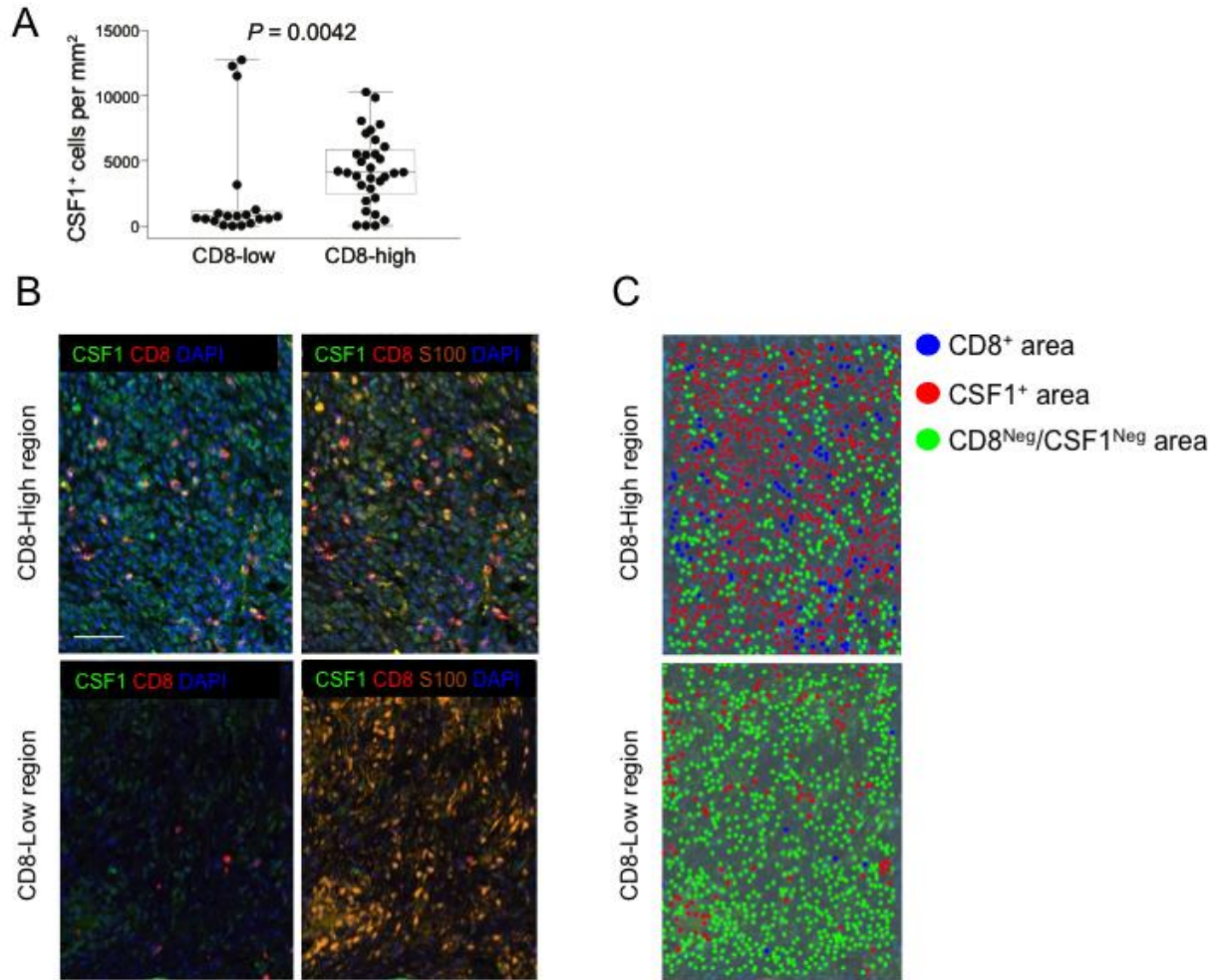


Fig. S3. CSF1⁺ cell density in high and low CD8⁺ cell-infiltrated tumor regions.

(A) Immunofluorescence analysis of primary tumors (N=3) and metastases (N=3) of cutaneous melanoma; for details, see **Table S1**. Tumor sections were stained with antibodies specific for CSF1, CD8 or S100, and with DAPI to reveal cell nuclei. CSF1-expressing cells were quantified in randomly selected (unpaired) CD8-low (N=19) and CD8-high (N=32) intratumoral regions. Error bars indicate min and max values. Statistical analysis by Mann-Whitney test. (B) Representative images of the immunofluorescence staining used for quantification of the data. Scale bar, 100 μ m. (C) Cell phenotype map identifying the cell populations defined by the individual markers in the 4-plex staining, overlaid on the raw image.

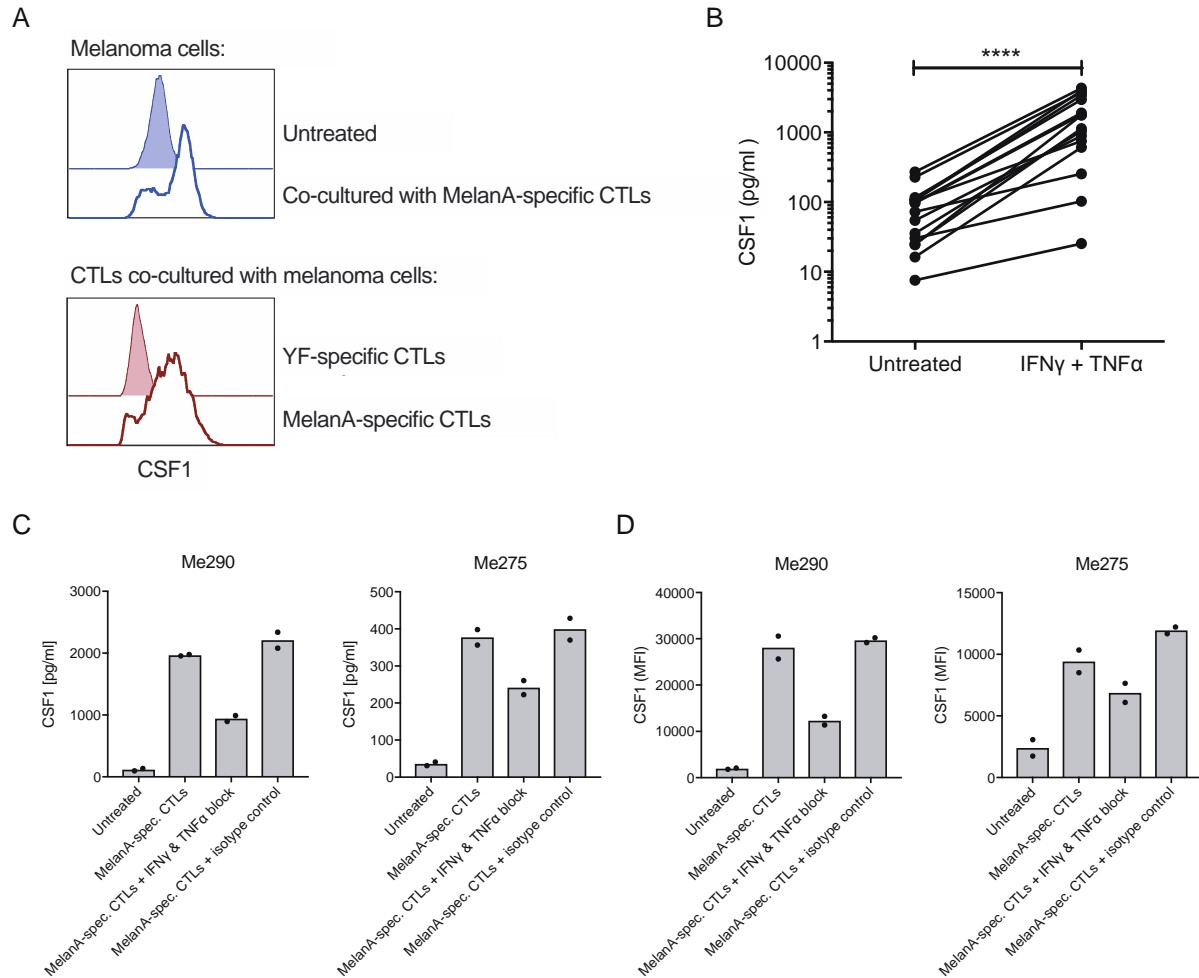


Fig. S4. CSF1 expression by melanoma cell lines and CTLs.

(A) Representative histograms of intracellular CSF1 protein in the melanoma cell line Me275 (top) and in CTLs (bottom) after 48h of co-culture, assessed by flow cytometry. Antigen-specific co-cultures were performed with MelanA-specific CTLs, whereas non-antigen-specific co-cultures used yellow fever (YF) virus-specific CTLs. (B) ELISA-based quantification of CSF1 in supernatants of sixteen melanoma cell lines (see **Table S2**) cultured for 48h in the presence or absence of IFN γ plus TNF α . Each dot represents the mean value from two replicates per cell line. Statistical analysis by Wilcoxon matched-pairs signed rank test. (C, D) CSF1 protein in the melanoma cell lines Me290 and Me275, measured after 48h of co-culture with MelanA-specific CTLs in the presence of IFN γ - and TNF α -blocking antibodies (IFN γ &TNF α block) or isotype control IgG. Two independent cell cultures per cell line were analyzed. In panel (C), CSF1 was quantified by ELISA in the cell culture supernatant; each dot represents the mean of two technical quantifications of the same supernatant. In panel (D), intracellular CSF1 protein was analyzed by flow cytometry. MFI, median fluorescence intensity.

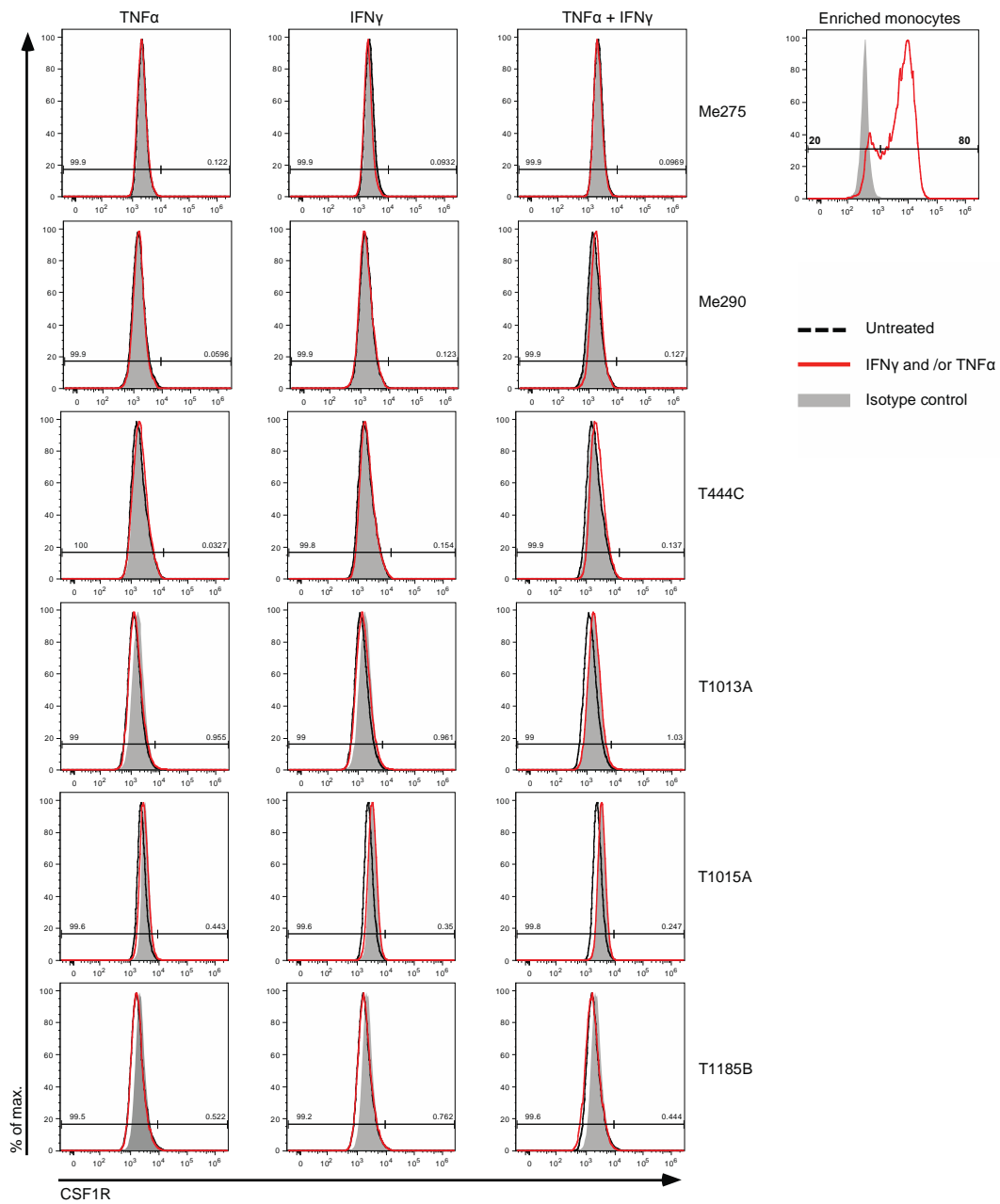


Fig. S5. Absence of CSF1R on the surface of untreated or cytokine-treated melanoma cell lines.

Six melanoma cell lines were left untreated (black dashed line) or treated with IFN γ , TNF α , or both, for two days (red solid line). Isotype IgG control is depicted in grey (filled line). Untreated monocytes enriched from human PBMCs were used as a positive control.

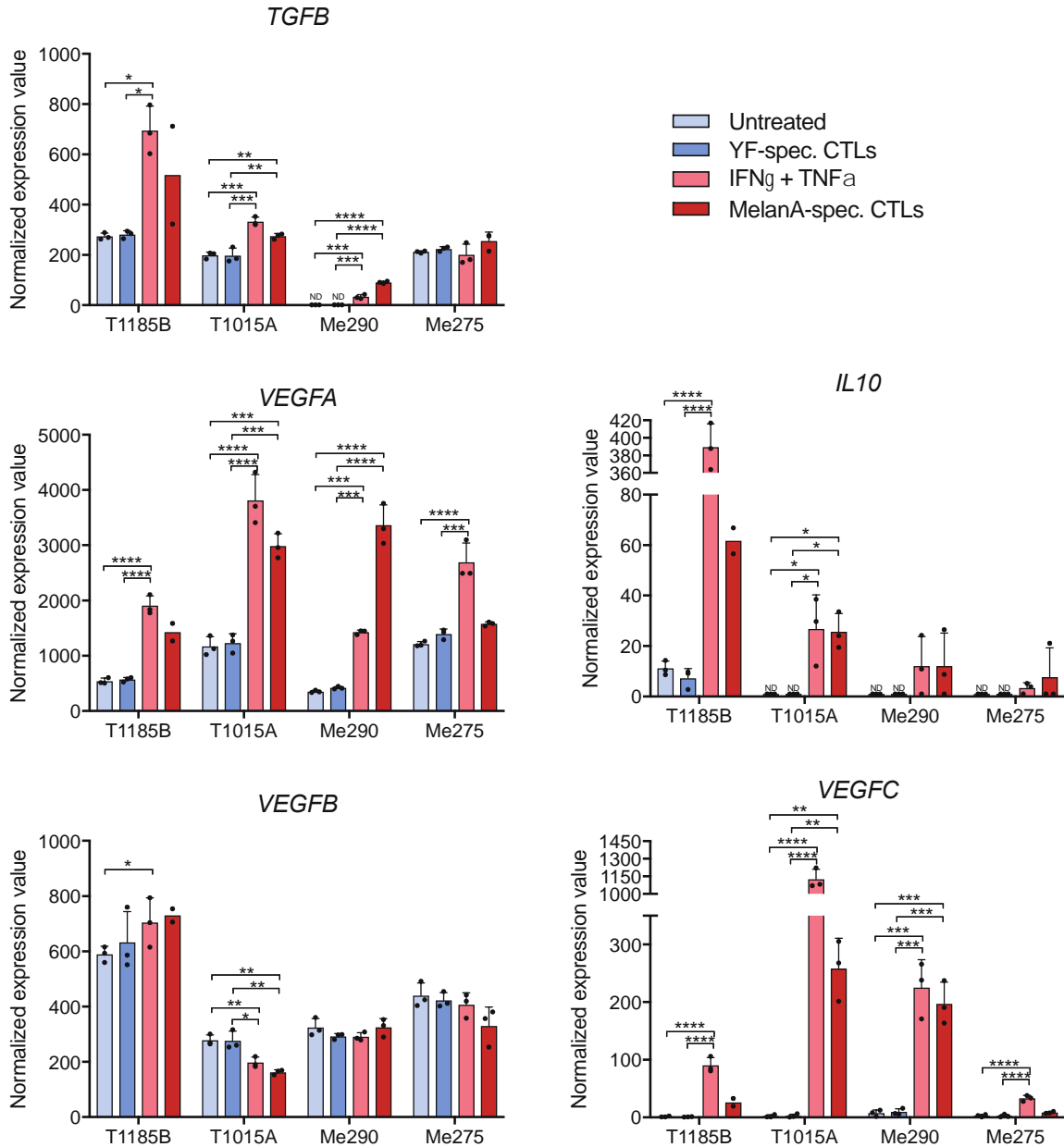


Fig. S6. Gene expression in human melanoma cells exposed to MelanA-specific CTLs or IFN γ and TNF α . Shown are the normalized expression values of *TGFB*, *IL10*, *VEGFA*, *VEGFB* and *VEGFC* mRNA in melanoma cells analyzed by NanoString 24h after the indicated treatment. For each cell line, three independent cell cultures per cell line are shown, except for T1185B of which two independent cell cultures were analyzed for melanoma cells cultured with MelanA-specific CTLs. For source data and description, please see references (48, 49). Statistical analysis by one-way ANOVA with correction for multiple comparisons by Tukey's test. ND, not detectable. Statistical significance: **** p<0.0001; *** p<0.001; ** p<0.01; * p<0.05.

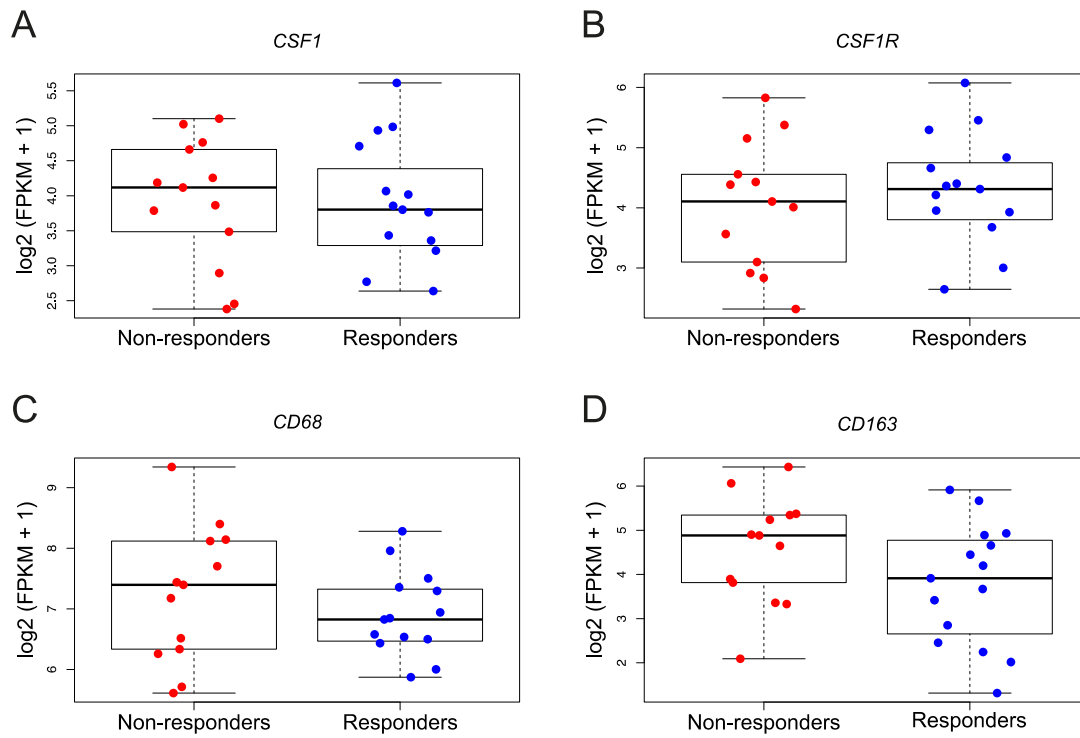


Fig. S7. Expression of macrophage genes in a transcriptomic data set of human melanoma treated with anti-PD1 therapy.

Expression of *CSF1* (A), *CSF1R* (B), *CD68* (C), and *CD163* (D) in melanomas of patients classified either as responder (N=15) or non-responder (N=13) to anti-PD1 therapy. There were no statistically significant differences. Data were extracted from Ref. (56).

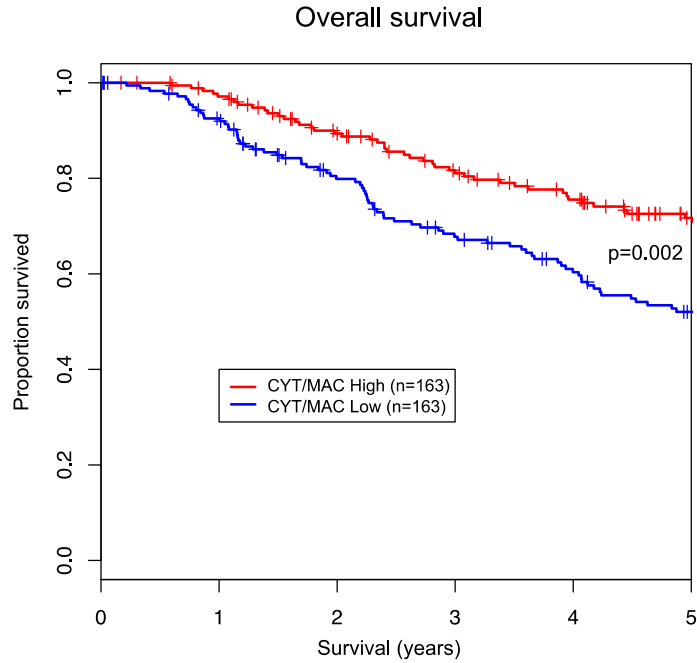


Fig. S8. Impact of CTL and TAM infiltrates on melanoma prognosis.

Kaplan-Meier estimate of survival in the SKCM metastatic cohort (N=326) of TCGA (46), stratified as high CYT/MAC ratio (N=163) or low CYT/MAC ratio (N=163) using median ratio as cutoff value. The CYT/MAC ratio denotes the numeric difference between log-transformed expression data. Cytotoxic T cell (CYT) score was defined as the geometric mean of *GZMA* and *PRF1* expression values. Likewise, macrophage (MAC) score was defined as the geometric mean of *CD68* and *CD163* expression values. Statistical analysis by log-rank test. *P* value was adjusted for tumor stage.

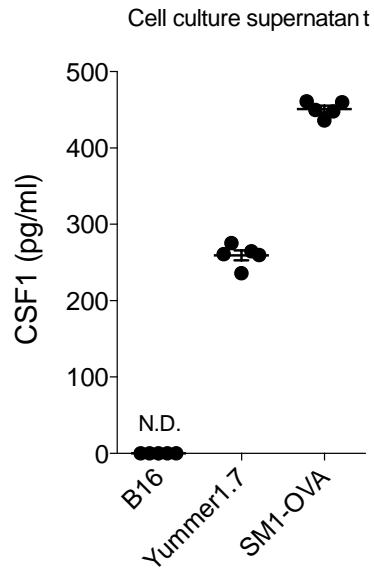


Fig. S9. Concentration of CSF1 in cell culture medium conditioned by mouse melanoma cells.

Concentration of CSF1 in cell culture medium conditioned for 48h by B16 (N=5), Yummer1.7 (N=5), or SM1-OVA (N=5) mouse melanoma cell lines. CSF1 concentration was determined by ELISA. Each dot represents one independent cell culture.

Supplementary Tables

Table S1. Melanoma patients, clinical parameters, and specimens analyzed in this study.

Patient	Gender ^a	Disease ^b	Stage/TNM at diagnosis	Date of specimen withdrawal	Stage/TNM at time of specimen withdrawal	Therapies before specimen withdrawal ^c	Clinical findings before specimen withdrawal	Specimen type ^d	Tumor localization	Analyzed in Figure(s) ^e
LAU205	M	SSM	IIIB/ pT2a N1b M0	19.01.2004	IIIB/ pT2a N2c M0	Surgery: excision of primary left pretibial lesion (22.05.1996)+ resection of one left inguinal LN metastasis (11.06.1996) + left inguino-crural and iliac radical lymphadenectomy (0N ⁺ , 26.06.1996); IFNalpha adjuvant (January to March 1998); Surgery: excision of an unique in transit metastasis on left thigh (02.12.2003)	In transit metastasis on left thigh (2003); relapse with in transit metastasis on the scar of the in transit metastasis (October 2007)	serum	NA	1C
				04.09.2008	IV/ pT2a N2c M1c	Additional therapies following the ones indicated above for this patient: Vaccines (a, January to November 2004; b, March 2005 to January 2007); Immunotherapy with lymphodepletion (c, November 2007-April 2008); Surgery: Wedge resection of right pulmonary lesion (09.05.2008)+ resection of one subcutaneous metastasis on left flank (13.06.2008); Radiotherapy on left sacro-iliac metastasis (15.07.2008)	Additional findings following the ones indicated above for this patient: 1 lung metastasis on right pulmonary lobe (PET.CT scan 28.04 2008)+ bone metastasis on ileo-sacral articulation and distant subcutaneous lesion under right scapula (PET-CT scan 27.06.2008)			
LAU392	F	SSM	IIA/ pT3a cN0 M0	15.08.2002	IIIC/ pT3a N3 cM0	Surgery: excision of primary lumbar lesion (18.04.1996)+ excision left axillary LN metastasis (03.02.2000)+ left axillary radical lymphadenectomy (8N ⁺ /16) and resection of a subcutaneous thoracic lesion (01.03.2000); Vaccine (d, April 2000 to August 2002); Surgery: excision subcutaneous metastasis on back (05.06.2001) + excision muscular lesion on back and 3 axillary LN metastases (21.12.2001); Radiotherapy post-surgery left axillary (60 Gy, 13.02 to 27.03.2002)	Left axillary LN suspect (CT-scan 24.02.2000); left axillary LN metastasis (CT-scan 13.02.2001); subcutaneous metastasis on back (June 2001); muscular metastasis on back and axillary LN metastases (December 2001)	serum	NA	1C
LAU465	M	SSM	IIA/ pT2b N0 M0	20.07.2010	IIIC/ pT2b N2c M0	Surgery: excision of primary scapular lesion (05.08.1994) + excision in transit subcutaneous metastasis in the back (23.08.2000) with axillary lymphadenectomy (0N ⁺ /16); Vaccine (e, 20 vaccinations, 31.10.2000 to 01.05.2003)	Subcutaneous metastatic nodule near left axillary area (cytoponction 09.08.2000)	serum	NA	1C
				10.11.2011	IIIC/ pT2b N2c M0	Additional therapies following the ones indicated above for this patient: Vaccine (f, 9 vaccinations, 29.07.2010 to 22.03.2011)	NA			

Patient	Gender ^a	Disease ^b	Stage/TNM at diagnosis	Date of specimen withdrawal	Stage/TNM at time of specimen withdrawal	Therapies before specimen withdrawal ^c	Clinical findings before specimen withdrawal	Specimen type ^d	Tumor localization	Analyzed in Figure(s) ^e
LAU616	M	SSM	IIIB/ pT3a N1b M0	24.10.2013	IV/ pT2b N3 M1c	Surgery: excision of primary left lumbar lesion (24.05.2001)+ wide re-excision and excision right inguinal sentinel LN (SN ⁺ , 04.07.2001); Vaccine (g, 6 vaccinations, 26.07.2001 to 18.10.2001); Surgery: right inguino-crural and ilio-obturator LN dissection (ON ⁺ /10, 22.08.2001)+ excision of a right inguinal metastasis (16.11.2005); Vaccine (h, 7 vaccinations, 19.12.2005 to 10.07.2006); Surgery: left inguino-crural and ilio-obturator lymphadenectomies (8N ⁺ /8) and excision of 9 subcutaneous metastases (suprapubic and right inguinal, 26.07.2006); Vaccine (i, 36 vaccinations, 21.11.2006 to 10.04.2012); Radiotherapy on brain metastasis (left frontal, 20Gy, 18.03.2008); Surgery: excision of the left frontal metastasis (07.08.2008)+ excision thoracic subcutaneous metastasis (20.08.2009)+ excision thoracic subcutaneous nodule and left axillary LN dissection (1N ⁺ /11, 04.10.2012); Vaccine (f, 9 vaccinations, 29.01.2013 to 17.10.2013)	Subcutaneous subpubic metastases (US 10.05.2006, confirmed by ponction); left and right inguinal adenopathies (PET-CT 21.06.2006); left and right axillary adenopathies (01.03.2007); regression of axillary adenopathies (CT-scan 08.10.2007); appearance of a brain metastasis (left frontal, CT-scan and brain MRI 26.02.2008); decrease of size of the brain metastasis (brain MRI 14.04.2008) but then progression of the brain metastasis (MRI 18.07.2008); regression of the brain metastasis with radionecrosis (brain MRI 03.11.2008); improved status in brain with regression of radionecrosis and of the hypersignal (brain MRI 17.08.2009); Status post-resection of frontal metastasis without relapse and new lesion (brain MRI 19.10.2010); appearance of a left axillary adenopathy and increase in size of a thoracic subcutaneous nodule (CT-scan 14.06.2012); progression with increase of size and metabolism of the axillary adenopathy and the thoracic subcutaneous nodule (PET-CT 03.09.2012)	serum	NA	1C
LAU660	F	NM	IIA/ pT2b N0 M0	19.08.2004	IV/ pT2b N0 M1c	Surgery: excision primary lesion on left thigh (05.11.2001)+ wide re-excision and sentinel LN dissection (ON ⁺ , 05.12.2001)+ excision metastases on right thigh and right flank (01.04.2004)+ excision one brain metastasis and two subcutaneous metastases on left flank and left breast (21.05.2004); Vaccine (j, 3 vaccinations, 23.08.2004 to 18.08.2004)	Subcutaneous left thoracic nodule (CT-scan 30.04.2004); one metastatic cerebral lesion in the left parietal area (MRI brain 06.05.2004)	serum	NA	1C
				30.09.2004	IV/ pT2b N0 M1c	Additional therapies following the ones indicated above for this patient: NA	Additional findings following the ones indicated above for this patient: NA			
LAU701	F	melanoma uk	IIB/ pT3b N0 M0	02.10.2003	IIIC/ pT3b N2c M0	Surgery: excision primary lesion on left arm (11.03.2002) re-excision and sentinel LN dissection (ON ⁺ , 22.05.2002); ILP with high dose TNFalpha, IFNgamma and Melphalan (19.03.2003) on 3 in transit nodules on left elbow; Vaporisation with CO2 laser (07.08.2003) of 3 nodules on arm	3 in transit nodules on left elbow (February 2003) and 3 nodules on arm (July 2003)	serum	NA	1C
LAU818	M	melanoma uk	IIA/ pT3a N0 M0	30.05.2006	IIIB/ pT3a N2b M0	Surgery: excision of primary lesion on back (26.04.2000)+ bilateral axillary LN dissection (1N ⁺ /2 on right, 1N ⁺ /1 on left, 16.12.2002); Vaccine (k, 18 vaccines, 12.05.2003 to 17.01.2005); Surgery: excision left axillary macro-metastatic lesion (30.01.2004); Radiotherapy on left axillary area (30Gy); Immunotherapy with lymphodepletion (l, 9 vaccines, 01.03.2005 to 25.10.2005); Surgery: left axillary radical LN dissection (1N ⁺ /2, 19.04.2005)	Left axillary adenopathy (PET 28.01.2004); 4 left axillary adenopathies (US 03.05.2006) and presence of large mass of left axillary adenopathies and 2 masses on left arm (PET-CT 24.05.2006)	serum	NA	1C
LAU972	F	NM	IIIB/ pT2b N1a M0	02.06.2004	IIIB/ pT2b N1a M0	Surgery: excision of primary lesion on back (15.03.2004)+ wide re-excision and sentinel LN dissection (right axillary: ON ⁺ and right inguinal:	NA	serum	NA	1C

Patient	Gender ^a	Disease ^b	Stage/TNM at diagnosis	Date of specimen withdrawal	Stage/TNM at time of specimen withdrawal	Therapies before specimen withdrawal ^c	Clinical findings before specimen withdrawal	Specimen type ^d	Tumor localization	Analyzed in Figure(s) ^e
						1N ⁺ , 28.04.2004)+ right axillary radical lymphadenectomy (0N ⁺ /17, 26.05.2004)				
LAU975	M	NM	IIIB/ pT4a N1b M0	09.03.2005	IIIB/ pT4a N2c M0	Surgery: excision of primary pectoral lesion (03.03.2004)+ wide re-excision and axillary sentinel LN dissection (right: 1N ⁺ and 2 micrometastases, left: 0N ⁺ , 07.04.2004)	In transit cutaneous metastasis (09.03.2005)	serum	NA	1C
LAU1013	M	ALM	IIIC/ pT3b N3 M0	09.01.2006	IV/ pT3b N3 M1a	Surgery: excision of primary lesion on left external malleolus (25.01.2005)+ wide re-excision and inguinal and iliac sentinel LN dissection (6N ⁺ /7, 23.02.2005)+ inguino-ilio-obturator lymphadenectomy (1N ⁺ /18, 03.03.2005); Vaccine (m, 8 vaccinations, 02.05.2005 to 09.01.2006); Surgery: excision of a cutaneous metastasis on left thigh (14.12.2005)	Distant cutaneous metastasis on left thigh (12.12.2005)	serum	NA	1C
LAU1017	F	NM	IIIC/ pT3b N2b M0	06.06.2005	IV/ pT3b N2b M1a	Surgery: excision of primary right paravertebral lesion (20.12.2004)+ wide re-excision and right axillary sentinel LN dissection (1N ⁺ micrometastasis, 09.02.2005)+ right axillary radical lymphadenectomy (1N ⁺ /9, 16.03.2005); Vaccine (m, 2 vaccinations injected, from 04.05.2005)	Relapse with a distant LN metastasis in left axillary hollow (PET-CT 29.04.2005)	serum	NA	1C
LAU1034	M	SSM	IIIB/ pT2a N2b M0	26.09.2005	IIIB/ pT2a N2b M0	Surgery: excision of primary right para-areolar lesion (21.03.2005)+ wide re-excision and left axillary sentinel LN dissection (2N ⁺ /2, 04.05.2005)+ left axillary radical lymphadenectomy (0N ⁺ /20, 15.06.2005); Vaccine (j, 2 vaccinations injected, from 15.08.2005)	NA	serum	NA	1C
LAU1090	M	NM	IIIB/ pT3a N2b M0	23.08.2007	IV/ pT3a N2b M1b	Surgery: excision of left paralumbar primary lesion (07.10.2005)+ wide re-excision and left axillary sentinel LN dissection (3N ⁺ /4, 07.12.2005)+ left axillary radical lymphadenectomy (0N ⁺ /17, 11.01.2006); Vaccine (j, 16 vaccinations, 06.03.2006 to 07.08.2007)	Relapse with 2 lung metastases in right pulmonary lobe (CT-scan 15.06.2006); progression in size of a right hilar adenopathy (CT-scan 02.04.2007)	serum	NA	1C
LAU1129	M	SSM	II/ pT3 N0 M0	08.03.2007	IIIC/ pT3 N3 M0	Surgery: excision of primary lesion on left thigh (07.09.1992)+ excision of left inguinal LN metastases (May 1993 and October 1993); Cisplatin+ Dacarbazine+ Methotrexate (12 cures, November 1993 to January 1994); Surgery: excision of an in transit metastasis (April 1998)+ excision of a left iliac LN metastasis (06.04.2006); Vaccine (b, 8 vaccinations, 10.07.2006 to 08.03.2007)	Regional LN metastases (3 inguinal N+, May and October 1993); in transit metastasis on the primary excision site (April 1998); regional LN metastasis (1 iliac N+, April 2006)	serum	NA	1C
LAU1131	F	melanoma uk	IIC/ pT4b N0 M0	08.05.2006	IIC/ pT4b N0 M0	NA	NA	primary tumor	scalp	2A, 2D (CSF1, CSF1R, CD163), 3B, S3
				09.08.2011	IV/ pT4b N0 M1c	Surgery: excision of primary lesion on scalp (08.05.2006) + wide re-excision and right retro-auricular sentinel LN dissection (26.06.2006, 0N ⁺ /2); Vaccines (n, 6 vaccinations, 31.08.2006 to 07.12.2006; c, 7 vaccinations, 21.02.2011 to 10.05.2011)	Hepatic and bilateral pulmonary metastases (CT-scan 30.11.2010 and biopsy in liver and lung on 09.12.2010 and 30.12.2010, respectively); progression of hepatic and pulmonary metastases (CT-scan 19.07.2011)	plasma/ serum	NA	1A, 1B

Patient	Gender ^a	Disease ^b	Stage/TNM at diagnosis	Date of specimen withdrawal	Stage/TNM at time of specimen withdrawal	Therapies before specimen withdrawal ^c	Clinical findings before specimen withdrawal	Specimen type ^d	Tumor localization	Analyzed in Figure(s) ^e
LAU1142	M	SSM	IA/ pT1a N0 M0	07.12.2010	IIIC/ pT1a N3 M0	Surgery: excision of left paralumbar primary lesion (01.11.2001)+ excision of 2 in transit right paralumbar metastases (31.05.2006)+ right inguino-crural lymphadenectomy (1N ⁺ /4) and excision of in transit right paralumbar metastasis (02.08.2006); Radiotherapy (42 Gy on right paralumbar area and 50.4 Gy on right inguinal area, 12.10.2006 to 21.11.2006); Vaccine (n, 7 vaccinations, 14.10.2008 to 12.03.2009)	Relapse with in transit paralumbar metastases (May 2006) and local progression with in transit metastases and one right inguinal LN metastasis (PET-CT 05.07.2006)	serum	NA	1C
LAU1144	M	NeM	IIA/ pT3a N0 M0	18.06.2007	IV/ pT3a N0 M1b	Surgery: excision of primary lesion on the nose (19.05.2003)+ excision of a pulmonary metastasis in the left lung (02.08.2006); Vaccine (b, 8 vaccinations, 28.09.2006 to 12.06.2007)	Relapse with one lung metastasis (PET-CT 26.06.2006)	serum	NA	1C
LAU1187	M	NM	IIIB/ pT2b N1a M0	05.08.2010	IIIB/ pT2b N1a M0	Surgery: excision of primary lesion on the left shoulder (06.12.2006)+ wide re-excision of the lesion and left axillary sentinel LN dissection (1N ⁺ /3, micrometastasis, 31.01.2007)+ left axillary radical lymphadenectomy (0N ⁺ /11, 13.04.2007); Vaccine (o, 16 vaccinations 26.06.2007 to 11.06.2009)	NA	serum	NA	1C
				24.06.2011	IIIB/ pT2b N1a M0	Additional therapies following the one indicated above for this patient: Vaccine (f, 9 vaccinations, 17.08.2010 to 16.06.2011)	NA			
LAU1189	F	ALM	IIIB/ pT3b N2 M0	05.06.2007	IIIB/ pT3b N2 M0	Surgery: excision of primary lesion on first toe of right feet (08.01.2007)+ re-excision of the primary lesion and right inguinal sentinel LN dissection (3N ⁺ /3, 07.02.2007)+ right inguino-crural radical lymphadenectomy (0N ⁺ /7, 27.04.2007)	NA	serum	NA	1C
LAU1268	M	melanoma uk	IIA/ pT3 N0 M0	15.06.2010	IIIC/ pT3 N3 M0	Surgery: excision of primary lesion on left leg (01.09.2004)+ wide re-excision of primary lesion and left inguinal sentinel LN dissection (0N ⁺ /2, 04.10.2004)+ excision of 2 in transit metastases on left leg (06.01.2006); Temodal (September 2007); Surgery: left inguino-crural radical lymphadenectomy (4N ⁺ /10, 19.11.2007) Vaccine (n, 7 vaccinations 12.06.2008 to 02.10.2008)	Relapse with in transit skin metastases (January 2006) and LN metastases (>4N ⁺ , November 2007); local relapse (1 left iliac metastasis and 1 left inguinal metastasis in the area of LN dissection, PET 29.09.2009)	serum	NA	1C
				09.06.2011	IV/ pT3 N3 M1a	Additional therapies following the one indicated above for this patient: Vaccine (f, 9 vaccinations, 22.06.2010 to 31.05.2011)	Additional findings following the ones indicated above for this patient: Distant skin metastasis in the left arm (US and biopsy 10.01.2011)			
LAU1273	F	NM	IA/ pT1a N0 M0	13.10.2009	IIIB/ pT1a N2c M0	Surgery: excision of cutaneous metastasis on left ankle (03.09.2007)+ left inguinal sentinel LN dissection (negative) and wide re-excision of primary lesion (28.11.2007); Adjuvant radiotherapy 30Gy (01.01.2008); Surgery: excision of an in transit metastasis on left knee (03.08.2009)	Presence of a subcutaneous metastatic nodule in the internal face of knee (PET-CT 26.08.2009)	metastasis	left limb	3B
				08.02.2011	IV/ pT1a N2c M1a	Additional therapies following the ones indicated above for this patient: Surgery: excision of 6 subcutaneous metastases on left ankle and of 2 LN metastases in the internal face of left knee (13.10.2009)+ excision of a metastasis on internal face of left calf (21.06.2010)+ excision of multiple in transit metastases on left leg (03.09.2010)+ excision of 5 new in transit metastases on calf and ankle (22.10.2010); DTIC: 2 cures (23.11 to	Additional findings following the ones indicated above for this patient: Apparition of a lesion in internal face of left ankle, a nodular lesion on right leg, a tissue nodule in the left flank (CT-scan 10.11.2010); Increase in number and size of the subcutaneous nodules in the left flank and in the subcutaneous tissue in left pre-	serum	NA	1B

Patient	Gender ^a	Disease ^b	Stage/TNM at diagnosis	Date of specimen withdrawal	Stage/TNM at time of specimen withdrawal	Therapies before specimen withdrawal ^c	Clinical findings before specimen withdrawal	Specimen type ^d	Tumor localization	Analyzed in Figure(s) ^e
						14.12.2010)	pectoral (CT-scan 18.01.2011)			
LAU1283	M	NM	IIIB/ pT4b N2a M0	14.04.2008	IIIB/ pT4b N2a M0	NA	NA	primary tumor	right pectoral area	2A, 2D (CSF1, CSF1R, CD163), 3B (S2, S3), S3 (S2, S3)
				22.03.2010	IIIC/ pT4b N2c M0	Surgery: excision of primary tumor on right pectoral (14.04.2008)+ wide re-excision and axillary sentinel LN dissection (1N ⁺ , 22.05.2008) + right axillary radical lymphadenectomy (1N ⁺ /7, 11.06.2008)+ resection of a local in transit metastasis (09.06.2009)+ resection of an in transit thoracic metastasis (07.10.2009 and 11.11.2009); Radiotherapy (5 fractions of 6 Gy, ended 25.01.2010)	Presence of 4 subcutaneous nodules in the right chest muscle and one mammary lesion (PET-CT 04.06.2009); Presence of 3 in transit metastases (2 right pectoral and 1 thoracic right lateral) (PET-CT 20.10.2009); Tumoral relapse in the right thoracic wall (3 subcutaneous nodules) (PET-CT 18.02.2010)	metastasis	trunk	2A, 2B, 2D (CSF1, CSF1R, CD163), 3A, 3B (S1), S3 (S1)
				09.12.2010	IV/ pT4b N2c M1c	Additional therapies following the ones indicated above for this patient: Surgery: excision of several right thoracic metastases (03.03.2010 and 22.03.2010); Adjuvant radiotherapy by tomotherapy (5 fractions of 6 Gy, ended 18.05.2010); Dacarbazine (25.08.2010 to 28.09.2010, 3 cycles)	Additional findings following the ones indicated above for this patient: Apparition of 2 in transit subcutaneous metastases on the right latero-thoracic area (CT 04.08.2010); Disease progression on thoracic area and duodenal wall (CT-scan 15.11.2010)	plasma/ serum	NA	1A, 1B
LAU1306	M	SSM	IIIB/ pT4a N2b M0	16.06.2010	IIIB/ pT4a N2c M0	Surgery: resection of primary lesion on left flank (18.08.2008)+ left axillary sentinel LN dissection (2N ⁺ /2)+ left axillary radical lymphadenectomy (0N ⁺ /11, 03.12.2008)+ excision of a local metastasis on left flank (19.05.2010)	Local relapse on the scar left flank (PET-CT-scan 10.05.2010)	metastasis	trunk	2A
				16.12.2010	IV/ pT4a N3 M1a	Additional therapies following the ones indicated above for this patient: Surgery: excision of residual melanoma on left flank and of a metastasis on left pectoral area (16.06.2010); Dacarbazine (3 cycles, 17.09.2010 to 28.10.2010)	Additional findings following the ones indicated above for this patient: Local relapse on anterior trunk and in the left flank with several in transit metastases in cutaneous, subcutaneous and muscular level (CT-scan 06.09.2010); Multiples subcutaneous metastases on trunk, left flank with a new left inguinal adenopathy (CT-scan 09.11.2010)	plasma/ serum	NA	1A, 1B
				16.05.2011	IV/ pT4a N3 M1a	Additional therapies following the ones indicated above for this patient: Ipilimumab (16.12.2010 to 08.03.2011, 3 cycles)	Additional findings following the ones indicated above for this patient: Regression of the left latero-thoracic lesions (CT-scan 21.03.2011)	metastasis	left pectoral area	2D (CSF1, CSF1R, CD163), 3B

Patient	Gender ^a	Disease ^b	Stage/TNM at diagnosis	Date of specimen withdrawal	Stage/TNM at time of specimen withdrawal	Therapies before specimen withdrawal ^c	Clinical findings before specimen withdrawal	Specimen type ^d	Tumor localization	Analyzed in Figure(s) ^e
LAU1314	M	melanoma uk	IIIC/ pT3b N1b M0	09.12.2010	IV/ pT3b N3 M1a	Surgery: excision of primary lesion on right leg (07.05.2008)+ wide re-excision of the lesion and inguinal sentinel LN dissection (positive, 10.10.2008)+ right inguinal radical lymphadenectomy (1N ⁺ /12, 07.01.2009)+ right ilio-obturator lymphadenectomy (3N ⁺ /5) and excision of a subcutaneous metastasis in left knee (24.03.2010)+ excision of 2 in transit lesions on knee and left leg and of a distant lesion on right arm (18.06.2010)	Relapse with right iliac adenopathies and in transit metastasis in left knee (March 2010); relapse with new in transit skin metastases and 1 distant skin metastasis (June 2010)	serum	NA	1C
				23.04.2013	IV/ pT3b N3 M1c	Vaccine (f, 9 vaccinations, 16.12.2010 to 04.10.2011)	Additional findings following the ones indicated above for this patient: right retrorenal adenopathy (biopsy 25.03.2013: metastasis); right subrenal mass, retroperitoneal LN metastases and lung metastasis (PET-CT 22.04.2013)			
LAU1342	F	melanoma uk	IIIC/ pTx N3 M0	14.10.2010	IIIC/ pTx N3 M0	Surgery: excision of in transit metastasis in left popliteal hollow with LN metastasis (31.03.2009)+ excision of a right paralobar metastatic nodule (26.08.2010); Vaccine (f, 9 vaccinations, 26.08.2010 to 12.05.2011)	Three in transit subcutaneous metastases (CT-scan 16.08.2010)	serum	NA	1C
				24.11.2011	IV/ pTx N3 M1a	Additional therapies following the ones indicated above for this patient: Surgery: excision of a right paralobar LN metastasis (31.05.2011)	Additional findings following the ones indicated above for this patient: right paralobar metastatic lesion (CT-scan 28.01.2011 and biopsy 04.04.2011)			
LAU1355	F	SSM	II/ pT3 N0 M0	31.05.2011	IV/ pT3 N2c M1c	Surgery: excision of primary lesion on right calf (07.04.2000) and wide re-excision (03.05.2000) + excision of about 20 in transit metastases on right leg (between 2005 and 2008); ILP with high dose TNFalpha, IFNgamma and Melphalan on right leg (26.08.2009); Surgery: right ilio-obturator lymphadenectomy (26.08.2009, 0N ⁺ /4); Dacarbazine (10 cures, 27.07.2010 to 08.02.2011); Surgery: resection of an in transit subcutaneous lesion on right leg (28.03.2011)	Apparition of several in transit subcutaneous metastases on right calf (January 2005); apparition of at least 9 new subcutaneous nodules on right calf without inguinal or popliteal LN metastasis (July 2009); local progression with metabolism increase of multiple known in transit subcutaneous metastases on right leg and foot and apparition of new nodules in right ankle (PET-CT 16.06.2010); Presence of two inguinal adenomegalies and a cerebral temporo-parietal nodule suspected of a metastasis (PET-CT 23.05.2011) confirmed with a complementary MRI: presence of 3 cerebral metastases (brain MRI 08.06.2011)	plasma	NA	1A
LAU1366	M	LMM	IB/ pT1b Nx Mx	15.07.2010	IV/ pT1b N2 M1c	Surgery: excision of primary lesion on scalp (22.04.2008); Cisplatin: chemoembolization of the liver (24.09.2009 and 15.12.2009); Surgery: excision of ileal lesion with LN metastases (2N ⁺ /7, 20.06.2010)	Hepatic metastasis (biopsy 31.08.2009); regression of hepatic metastasis (abdominal MRI 26.10.2009 and 30.04.2010); tumoral lesion in ileum (PET-CT 25.05.2010)	serum	NA	1C
				19.01.2012	IV/ pT1b N2 M1c	Additional therapies following the ones indicated above for this patient: Vaccine (f, 9 vaccinations, 22.07.2010 to 30.03.2011)	Additional findings following the ones indicated above for this patient: NA			

Patient	Gender ^a	Disease ^b	Stage/TNM at diagnosis	Date of specimen withdrawal	Stage/TNM at time of specimen withdrawal	Therapies before specimen withdrawal ^c	Clinical findings before specimen withdrawal	Specimen type ^d	Tumor localization	Analyzed in Figure(s) ^e
LAU1394	M	SSM	IIA/ pT3 pN0 M0	13.03.2012	IV/ pT3 pN2b M1c	Surgery: excision of primary tumor on right thigh (04.11.2008) + right inguinal sentinel LN dissection (0N ⁺ /3, 17.12.2008)+ right inguino-crural radical lymphadenectomy (2N ⁺ /7) and excision of Cloquet LN (1N ⁺ /1) (05.05.2010); Radiotherapy by tomography (total dose of 30Gy) on inguinal area (21 to 30.07.2010); Surgery: right ilio-obturator and right paracave lymphadenectomies (1N ⁺ /19, 09.11.2010); Vaccine (p, 4 vaccines, 15.03.2011 to 07.06.2011); Surgery: resection of a left adrenal metastasis (08.09.2011); Temodal (2 cycles, 26.12.2011 to 22.02.2012); Radiotherapy by stereotaxy on the posterior parietal metastasis (24.01.2012)	Right inguinal adenopathy (biopsy positive 12.03.2010); several LN metastases (right external iliac, mesenteric, retro-peritoneal and para-renal left) (PET-CT 25.11.2011); disease progression with multiple hypermetabolic cerebral lesions (MRI brain 08.12.2011); disease progression with new adenopathies (iliac, mesenteric, retroperitoneal, subclavicular) and subcutaneous nodules on left thigh (PET-CT 22.02.2012)	plasma/ serum	NA	1A, 1B
LAU1397	F	melanoma uk	III/ Tx cN3 cM0	19.01.2011	III/ Tx N3 cM0	Surgery: excision of primary tumor on left arm (1998)+ left axillary radical lymphadenectomy (11N ⁺ /14, 31.03.2010); Radiotherapy by tomography on metastasectomy bed (5 fractions of 6 Gy, completed on 22.06.2010); Vaccine (p, 8 vaccines, 05.10.2010 to 20.05.2011)	Presence of hypermetabolic left axillary adenopathies (PET-CT 26.03.2010)	plasma/ serum	NA	1A, 1B
LAU1407	M	NM	IIB or III/ pT4a Nx Mx	22.02.2011	IV/ pT4a pN1b M1c	Surgery: resection of primary dorsal lesion (28.07.2008)+ Axillary left radical lymphadenectomy (1N ⁺ /7) and complementary excision of primary lesion (13.08.2009); Radiotherapy of axillary area (ended in Dec. 2009); Protocol BRIM3: Vemurafenib (11 cycles, 15.06.2010 to 11.01.2011)	Relapse with axillary LN metastases (biopsy 10.07.2009); progression with multiple distant metastases (axillary, subcutaneous, pulmonary, renal, surrenal, hepatic, retroperitoneal; CT-scan 10.06.2010); progression with new lesions in left renal parenchyme and retroperitoneal adenopathy and increase of hyperactivity of the known metastatic lesions (PET-CET 14.01.2011)	serum	NA	1B
				01.02.2012	IV/ pT4a pN1b M1c	Additional therapies following the ones indicated above for this patient: Ipilimumab (4 cycles, 22.02.2011 to 05.04.2011); Radiotherapy all brain (27.07 to 10.08.2011)+ Temodal; Vemurafenib (reinduction 04.11.2011 to 18.11.2011)	Additional findings following the ones indicated above for this patient: Progression (brain, LN, pulmonary, surrenal, subcutaneous; CT-scan 25.05.2011); cerebral progression (increase in size of 5 metastases; MRI brain 30.09.2011); decrease of known metastases (CT-scan 16.11.2011 and MRI brain 17.11.2011)	metastasis	external face right arm	2A, 2D (CSF1, CSF1R, CD163), 3B
LAU1416	M	NM	IB/ pT2a cN0 cM0	21.09.2010	IIIC/ pT2a pN3 M0	Surgery: excision of primary lesion on anterior face left thigh (06.07.2005)+ excision subcutaneous metastasis on left thigh (31.05.2010)+ left inguino-crural radical lymphadenectomy (6N ⁺ /9, 21.07.2010)	Relapse with inguino-crural LN metastases (July 2010)	metastasis	left thigh	2D (CSF1, CD163)
				11.01.2011	IIIC/ pT2a pN3 M0	Additional therapies following the ones indicated above for this patient: Surgery: excision cutaneous metastasis on left thigh (21.09.2010); Dacarbazine (1 cure, 30.11.2010)	Additional findings following the ones indicated above for this patient: Cutaneous relapse in left thigh (September 2010); Clinical progression with increase of lesions in left thigh (21.12.2010)	serum	NA	1B

Patient	Gender ^a	Disease ^b	Stage/TNM at diagnosis	Date of specimen withdrawal	Stage/TNM at time of specimen withdrawal	Therapies before specimen withdrawal ^c	Clinical findings before specimen withdrawal	Specimen type ^d	Tumor localization	Analyzed in Figure(s) ^e
LAU1419	M	NM	IB/ pT2a N0	26.06.2012	IV/ pT2a N2b M1c	Surgery: primary excision on left calf (12.09.2008)+ left inguinal sentinel LN dissection (0N ⁺ /2, 07.01.2009)+ excision in transit metastasis on left calf (31.05.2010)+ left ilio-inguinal lymphadenectomy (1N ⁺ /3) and left ilio-obturator lymphadenectomy (1N ⁺ /8) (21.11.2011)	Relapse with in transit metastasis on left calf (May 2010); relapse with inguinal/ internal obturator LN metastases (PET-CT 13.10.2011); progression with one metastasis in abdomen and two in transit metastases on left calf (PET-CT 23.05.2012)	metastasis	calf	2D (CSFIR, CD163)
				02.07.2013	IV/ pT2a N2b M1c	Additional therapies following the ones indicated above for this patient: Surgery: excision of metastases in proximal jejunum and of in transit lesions on left calf (26.06.2012); Radiotherapy by Gammaknife on cerebral metastases (17.10.12); Protocol Novartis CMEK 162X with treatment by MEK inhibitor (22.01.13 to 11.06.13)	Additional findings following the ones indicated above for this patient: Progression with cerebral metastases, subcutaneous metastasis in right thigh, and lombo-aortic and left iliac LN metastases (12.09.2012 PET-CT); Appearance of 2 cerebral metastases (MRI brain 04.10.2012); Intra-peritoneal and LN progression (after a partial response to the MEKi treatment) (PET-CT 10.06.2013)	plasma	NA	1A
LAU1422	M	ALM	IIB/ pT3b pN0 Mx	19.05.2011	IV/ pT3b cN3 M1c	Surgery: excision/biopsy of primary tumor on right heel (01.06.2010) + re-excision and right inguinal sentinel LN dissection (negative, 14.07.2010); Dacarbazine (2 cures, 10.02.2011 to 25.03.2011)	Appearance of LN metastases (right popliteal, right inguinal, iliac, retroperitoneal, retrocardiac; CT-scan 14.01.2011); LN progression (inguinal, iliac, retroperitoneal, peri/para-aortic; PET-CT 24.03.2011 and 18.05.2011)	plasma/ serum	NA	1A, 1B
LAU1438	F	SSM	IB/ T2 Nx Mx	17.05.2011	IV/ T2 Nx M1c	Surgery: excision of primary lesion on back (29.05.2002)+ biopsy of a bone metastasis in the left femur (27.09.2010) and tumorectomy with arthrodesis (22.10.2010) and prosthesis of the knee (07.12.2010)	Bone metastasis in the left distal femur (MRI knee 18.10.2010)	serum	NA	1C
				01.12.2011	IV/ T2 Nx M1c	Vaccine (f, 6 vaccinations 31.05.2011 to 25.11.2011)	Additional findings following the ones indicated above for this patient: NA			
LAU1444	F	NM	II/ pT3 N0 M0	14.12.2010	IV/ pT3 N0 M1c	Surgery: excision of primary tumor on first thumb of left foot (15.05.2001)+ left inguinal sentinel LN dissection (negative, May 2001)+ biopsy/excision of a metastasis in left mandibular angle (17.06.2010); DTIC: 3 cures (24.08 to 09.10.2010); Radiotherapy on the mandibular lesion (20Gy in 5 fractions of 4Gy, 02.12 to 08.12.2010)	Distant metastatic progression to left mandibule (June 2010) and bilateral pulmonary, hepatic, renal, bone and peritoneal level (PET-CT 19.10.2010)	plasma	NA	1A
LAU1456	F	SSM	IIIB/ pT3b N2b M0	28.04.2011	IIIB/ T3b N2b M0	Surgery: excision of primary tumor on right leg (05.11.2010)+ re-excision of the primary lesion and right inguinal sentinel LN dissection (1N ⁺ , 25.11.2010)+ right inguinal radical lymphadenectomy (1N ⁺ , 14.01.2011)	NA	serum	NA	1C
				04.07.2011	IIIC/ T3b N3 M0	Surgery: right inguino-crural lymphadenectomy (conglomerate metastasized and 1N ⁺ /3) and right ilio-obturator lymphadenectomy (3N ⁺ /12) (08.06.2011); Vaccine (f, 3 vaccinations, 05.05.2011 to 28.06.2011)	Right inguinal adenopathies (CT-scan 28.04.2011 and US/biopsy 10.05.2011)			

Patient	Gender ^a	Disease ^b	Stage/TNM at diagnosis	Date of specimen withdrawal	Stage/TNM at time of specimen withdrawal	Therapies before specimen withdrawal ^c	Clinical findings before specimen withdrawal	Specimen type ^d	Tumor localization	Analyzed in Figure(s) ^e
LAU1461	M	melanoma	IV/ Tx Nx M1c	24.03.2011	IV/ Tx Nx M1c	Surgery: biopsy of an abdominal mass between liver and colon; Temodal (3 cures, 23.11.2010 to 17.01.2011)	Tumoral mass between liver and colon, intraperitoneal LN, pulmonary, hepatic and thyroid metastases (PET-CT 29.10.2010); Progression of the abdominal mass, pulmonary, hepatic and intraperitoneal LN metastases and apparition of mediastinal and retroperitoneal adenopathies (CT-scan 07.02.2011)	plasma	NA	1A
LAU1477	F	NM	IIIA/ pT3a N1a M0	27.09.2011	IIIA/ T3a N1a M0	Surgery: excision of primary lesion on left ear (01.04.2009)+ wide re-excision of lesion and intra-parotidian sentinel LN dissection (1N ⁺ for micrometastasis, 07.05.2009)+ cervical lymphadenectomy (levels II to IV, 0N ⁺ /19) and excision of left parotide (05.08.2009)+ left cervical radical lymphadenectomy (levels III to V, 16.05.2011, 0N ⁺ /25)	Apparition adenopathies in left cervical levels III and V (US cervical and cytoponction with isolated tumoral cells, April 2011) but pathology negative on cervical LN excised (0N ⁺ /25, 16.05.2011)	serum	NA	1C
				17.07.2012	IIIA/ T3a N1a M0	Vaccine (f, 9 vaccinations, 04.10.2011 to 10.07.2012)	Additional findings following the ones indicated above for this patient: NA			
LAU1486	F	NM	IIB/ pT3b N0 M0	26.06.2012	IV/ pT3b N0 M1b	Surgery: excision of primary lesion on right arm (11.02.2009)+ wide re-excision of the lesion and right axillary sentinel LN dissection (0N ⁺ /3, 01.04.2009); complete excision of a pulmonary metastasis in the left superior lobe (16.12.2010); Radiotherapy on nodule in the right inferior pulmonary lobe (01.09.2011 and 24.01.2012)	Apparition of a parenchymal nodule in the left superior pulmonary lobe (PET-CT 02.11.2010); new relapse with nodule in the right inferior pulmonary lobe (13.07.2011)	serum	NA	1C
				27.03.2014	IV/ pT3b N0 M1b	Additional therapies following the ones indicated above for this patient: Vaccine (f, 9 vaccinations, 28.06.2012 to 21.02.2013)	Additional findings following the ones indicated above for this patient: NA			
LAU1488	M	ALM	IB/ pT2 pN0 M0	23.09.2011	IV/ pT2 pN0 M1b	Surgery: excision of primary tumor 1 st melanoma ALM (IB/ pT2 pN0 M0) on the scalp (06.01.2004)+ sentinel LN dissection (negative, 12.02.2004); excision of in situ paralumbar 2 nd melanoma SSM (0Tis,19.02.2008)+ re-excision of the scar (04.3.2008)	Progression with LN, pulmonary, muscular and cerebral metastases (CT-scan 16.09.2011);	metastasis	cervical	2A, 2D (CSF1, CSF1R), S3
				15.03.2012	IV/ pT2 pN0 M1c	Additional therapies following the ones indicated above for this patient: Surgery: biopsy/excision subcutaneous cervical metastasis of the scalp melanoma (23.09.2011); Radiotherapy brain concomitant with chemotherapy Temodal (18.10.2011 to 01.12.2011); Vemurafenib (4 cycles, 15.11.2011 to 08.03.2012)	Additional findings following the ones indicated above for this patient: Progression with increase in size of the known cerebral metastases (MRI brain 08.11.2011); Dissociate response with regression of cerebral and pulmonary metastases but progression of subcutaneous, intra-muscular and intra-peritoneal nodules (MRI/ PET-CT 05.03.2012)	plasma	NA	1A
LAU1498	M	NM	IIIB/ pT4b pN1a M0	12.02.2013	IV/ pT4b pN1a M1c	Surgery: excision of primary tumor on right scapula (20.07.2011)+ right axillary sentinel LN dissection (1N ⁺ : micrometastasis) and re-excision of the scar (12.10.2011)+ right axillary radical lymphadenectomy (0N ⁺ /19, 04.01.2012); Dacarbazine (6 cures,14.08.2012 to 06.12.2012)	Progression with lung metastases in right superior lobe and latero-tracheal LN metastases (CT-scan 09.07.2012); Progression with right retro-clavicular, right latero-tracheal LN, pulmonary, hepatic and iliac metastases , and 2 cerebral metastases (PET-CT/ MRI brain 24.01.2013)	plasma	NA	1A

Patient	Gender ^a	Disease ^b	Stage/TNM at diagnosis	Date of specimen withdrawal	Stage/TNM at time of specimen withdrawal	Therapies before specimen withdrawal ^c	Clinical findings before specimen withdrawal	Specimen type ^d	Tumor localization	Analyzed in Figure(s) ^e
				24.04.2014	IV/ pT4b pN1a M1c	Additional therapies following the ones indicated above for this patient: Ipilimumab (4 cures, 12.02.2013 to 16.04.2013); Radiosurgery: one dose 24 Gy on 3 cerebral metastases (27.02.2013); Radiotherapy Gammaknife on 2 new cerebral lesions (13.08.2013) and on 3 new cerebral lesions (10.04.2014)	Additional findings following the ones indicated above for this patient: Progression of a sus-clavicular adenopathy and 2 subcutaneous nodules (PET-CT 19.03.2013); Partial metabolic response of the metastasis with no appearance of new metastatic lesion (PET-CT 28.05.2013); Stability cerebellar lesions and decrease in size of a right insular lesion (MRI brain 18.04.2013); Progression of the LN, subcut, pulmo and cerebral lesions (PET-CT/ MRI brain 13.03.2014)	metastasis	right clavicle	2D (CSF1R, CD163)
LAU1499	M	ALM	IIIB/ pT4b pN1a M0	29.11.2011	IIIB/ pT4b pN1a M0	NA	NA	primary tumor	1st left foot toe	2A, 2D (CSF1, CSF1R, CD163)
				03.05.2012	IIIB/ pT4b N1a M0	Additional therapies following the ones indicated above for this patient: Surgery: excision of primary lesion in the toe of the left feet and left inguinal sentinel LN dissection (positive, 29.11.2011)+ left inguinal radical lymphadenectomy (0N ⁺ /12, 06.01.2012)	NA	serum	NA	1C
				05.02.2013	IIIB/ pT4b N1a M0	Additional therapies following the ones indicated above for this patient: Vaccine (f, 9 vaccinations, 08.05.2012 to 29.01.2013)	NA			
LAU1501	F	NM	IV/ T4b Nx M1c	08.11.2012	IV/ T4b Nx M1c	Surgery: excision of primary tumor on the back (17.10.2011); Vemurafenib (10.12.2011 to 27.09.2012); Radiotherapy Gammaknife on the thalamic lesion (09.02.2012) and on cerebral metastatic lesions (26.07.2012 and 18.10.2012)	Diaphragmatic adenopathies and hypermetabolic splenic and pulmonary nodules (PET-CT 27.10.2011); Appearance of a cerebral metastatic lesion on left thalamus (MRI brain 02.12.2011); Appearance of 3 new cerebral metastases (MRI brain 02.07.2012); Appearance of a new cerebral metastasis (MRI brain 18.09.2012); Appearance of left axillary LN metastasis and bilateral inguinal LN metastases (CT-scan 04.10.2012)	plasma	NA	1A
LAU1503	F	ALM	I/ pT1 N0 M0	09.02.2012	IV/ pT1 cN3 M1a	Surgery: excision of primary tumor on right heel (11.05.2005)+ re-excision lesion and scar (23.05.2005); Dacarbazine (2 cures, 08.12.2012 to 29.12.2011)	Appearance of multiple retroperitoneal iliac, inguinal LN metastases and presence of left retro-clavicular LN metastases (biopsy with needle in right inguinal LN 11.11.2011 and CT-scan 23.11.2011); New retrocrural LN metastases and progression of left sus-clavicular LN metastases and right retroperitoneal and iliac LN metastases (PET-CT 16.01.2012)	plasma	NA	1A
LAU1517	M	ALM	IIc/ T4b N0 M0	20.01.2011	IIc/ pT4b N0 M0	NA	NA	primary tumor	left thumb	3B, S3

Patient	Gender ^a	Disease ^b	Stage/TNM at diagnosis	Date of specimen withdrawal	Stage/TNM at time of specimen withdrawal	Therapies before specimen withdrawal ^c	Clinical findings before specimen withdrawal	Specimen type ^d	Tumor localization	Analyzed in Figure(s) ^e
				05.10.2012	IV/ pT4b N3 M1b	Surgery: excision of primary lesion on left thumb (20.01.2011)+ left axillary sentinel LN dissection (negative) and amputation left thumb (23.03.2011); Dacarbazine (4 cures, 24.01.2012 to 04.04.2012); Ipilimumab (03.05 to 14.06.2012, 3 cycles, stop due to grade 3 colitis)	Loco-regional in transit subcutaneous metastases in left arm and pulmonary metastatic progression with pulmonary nodules and hypermetabolic left hilar LN (CT-scan 10.01.2012 and 01.03.2012); locoregional and pulmonary progression after a good initial response to the treatment with Dacarbazine (PET-CT 18.04.2012); Partial response with decrease of some pulmonary and cutaneous lesions (week 12, treatment Ipilimumab; PET-CT 19.07.2012); and then metabolic progression of cutaneous and pulmonary known lesions (week 16, treatment Ipilimumab; PET-CT 16.08.2012)	metastasis	right lip	2A, 2D (CSF1, CSF1R, CD163)
LAU1542	M	SSM	IA/ pT1a cN0 cM0	20.06.2013	IV/ pT1a pN3 M1c	Surgery: biopsy of primary lesion (21.10.2010)+ re-excision of the primary tumor/ BRAF mutated (16.12.2010)+ left cervical lymphadenectomy (23.10.2012, 7N ⁺ /13)+ excision metastatic left subclavicular LN (05.11.2012); Radiotherapy (hypofractionated of a total dose of 30 Gy, from 17.12.12 to 02.01.13, subclavicular area and left latero-cervical); Radio-surgery with Linac (dose 24 Gy) on left temporal metastasis (22.04.13); Temozolomide (05.04.13 to 30.05.13, 2 cycles); Radio-surgery with Linac (dose 24 Gy) on the 2 cerebral metastases (10.06.13)	Subcutaneous and left cervical LN progression (cytoponction 11.09.2012); multiple cervical lymphadenopathies (CT-scan 21.09.2012); metastatic bilateral cervical nodal progression, left inguinal and subcutaneous (right pectoral) (PET-CT 07.03.2013) confirmed by pectoral and inguinal biopsy (11.03.2013); left antero-inferior temporal cerebral metastasis (MRI brain 21.03.2013); appearance of 2 new cerebral metastatic lesions (right superior parietal and in left post-central gyrus; MRI brain 27.05.13)	plasma	NA	1A
				11.11.2013	IV/ pT1a pN3 M1c	Additional therapies following the ones indicated above for this patient: Ipilimumab (20.06.2013 to 17.07.2013, 2 cycles); Vemurafenib (17.07 to 05.11.13)	Additional findings following the ones indicated above for this patient: Progression of the known lesions (CT-scan 17.07.2013); initial partial response to the treatment with Vemurafenib (PET-CT 10.09.2013) and progression of pectoral right lesion, inguinal right lesion and of a submandibular left nodule (PET-CT 16.10.2013)	metastasis	left sous-mandibular	2A, 2D (CSF1, CSF1R, CD163), S3
LAU1615	F	DM	IIA/ T3a N0 M0	05.08.2004	IIA/ T3a N0 M0	NA	NA	primary tumor	chin	2A
LAU1637	F	NM	IV/ pT3b pN2c M1	13.12.2013	IV/ pT3b pN2c M1	NA	NA	primary tumor	vulva	2A, 2D (CSF1, CSF1R, CD163)

NA, not applicable; ILP, Isolated limb perfusion; LN, lymph node; N⁺, metastatic LN; MRI, magnetic resonance imaging; PET-CT, positron emission tomography-computed tomography; US: ultrasound.

For Figure 1C, 13 patients provided sera at two different time points, at an earlier and subsequently at a more advanced disease stage.

^a M: male; F: female

^b ALM: acral lentiginous melanoma, DM: dermoplastic melanoma, LMM: lentigo maligna melanoma, NM: nodular melanoma, NeM: nevoid melanoma, SSM: superficial spreading melanoma,

melanoma uk: unknown type of melanoma

^c Vaccination therapies:

a: P40/ELA cancer vaccine study: Melan-A₂₆₋₃₅ (A27L) analog peptide (ELA)+ P40 adjuvant

b: LUDWIG 00-018 cancer vaccine study (group 4): CpG-7909/PF-3512676 + Melan-A₂₆₋₃₅ (A27L) analog peptide (ELA) + Tyrosinase peptide+ Montanide ISA-51

c: CePO ITA-02 adoptive transfer study (2nd amendment): lymphocytopheresis + lymphodepletion with Endoxan / Fludarabine + reinfusion of PBMCs and vaccine with Melan-A₂₆₋₃₅ (A27L) analog peptide (ELA)+ sLAG-3 Ig (ImmuFact® IMP321) + Montanide ISA-51

d: LUDWIG 96-010 cancer vaccine study: Melan-A₂₆₋₃₅ (A27L) analog peptide (ELA)+ FluMa₅₈₋₆₆ peptide + low dose rhIL-2+ SB AS-2

e: LUDWIG 96-010 cancer vaccine study: Melan-A₂₆₋₃₅ (A27L) analog peptide (ELA)+ FluMa₅₈₋₆₆ peptide + low dose rhIL-2+ Montanide ISA-51

f: LAG-3 cancer vaccine study: MAGE-A3₁₁₂₋₁₂₀ (MAGE-A3.A2)+ NY-ESO-1₁₅₇₋₁₆₅ peptide + Melan-A₂₆₋₃₅ (A26L) native peptide (EAA) in first cycle, then Melan-A₂₆₋₃₅ (A27L) analog peptide (ELA) in cycles 2 and 3+ NA-17 + MAGE-A3₂₄₃₋₂₅₈ (MAGE-A3.DP4 LP)+ sLAG-3 Ig (ImmuFact® IMP321) + Montanide ISA-51

g: LUDWIG 98-009 cancer vaccine study: Melan-A₂₆₋₃₅ (A27L) analog peptide (ELA)+MAGE-A10 peptide + SB AS-2

h: LUDWIG 01-003 cancer vaccine study (group 2): Melan-A₂₆₋₃₅ (A27L) analog peptide (ELA)+ MAGE-A10+ NY-ESO-1₁₅₇₋₁₆₅ + Montanide ISA-51

i: LUDWIG 01-003 cancer vaccine study (group 3) : Melan-A₂₆₋₃₅ (A27L) analog peptide (ELA)+ MAGE-A10+ NY-ESO-1₁₅₇₋₁₆₅ + Montanide ISA-51 + CpG-7909/PF-3512676

j: LUDWIG 00-018 cancer vaccine study (group 2): CpG-7909/PF-3512676 + Melan-A₂₆₋₃₅ (A26L) native peptide (EAA) + Montanide ISA-51

k: LUDWIG 00-018 cancer vaccine study (group 1): CpG-7909/PF-3512676 + Melan-A₂₆₋₃₅ (A27L) analog peptide (ELA) + Montanide ISA-51

l: CePO ITA-01 adoptive transfer study: lymphocytopheresis + lymphodepletion with Busulfan / Fludarabine + reinfusion of PBMCs and vaccine with Melan-A₂₆₋₃₅ (A27L) analog peptide (ELA)+ Montanide ISA-51

m: LUDWIG 00-018 cancer vaccine study (group 3): CpG-7909/PF-3512676 + Melan-A₂₆₋₃₅ (A26L) native peptide (EAA) + Tyrosinase peptide+ Montanide ISA-51

n: CYT004-MelQbG10 04 cancer vaccine study : Virus-like particles MelQbG10 (long Melan-A₁₆₋₃₅ (A27L) analog peptide) + Montanide ISA-51

o: LUDWIG 01-003 cancer vaccine study (group 1): Melan-A₂₆₋₃₅ (A27L) analog peptide (ELA)+ Montanide ISA-51

p: LUDWIG 01-003 cancer vaccine study (group 5): Melan-A₂₆₋₃₅ (A27L) analog peptide (ELA) + Melan-A EAA peptide + MAGE-A10 peptide + NY-ESO-1_{lp 79-108} (long peptide) + Montanide ISA-51 + CpG-7909/PF-3512676+ low dose rhIL-2

^d Specimen types: plasma/ serum (white background), primary melanoma (light grey background), melanoma metastasis (dark grey background)

^e The last column indicates the Figures containing data generated with specimens from the respective patients. The type of data may be enclosed in parentheses. (S1, S2, S3) in parentheses refer to the samples of patient LAU 1283 in Figure 3 / Figure S3.

Table S2. Origin of the melanoma cell lines used in this study.

Tumor cell line	Patient	Tumor type	Tumor localization	Used in Figures	Refs.
Me275	LAU50	Metastasis	lymph node	4, S4A/C/D, S5	(48, 49, 96-105)
Me290	LAU203	Metastasis	lymph node	4, S4C/D, S5	(48, 49, 98, 99, 103)
T1185B	LAU1185	Metastasis	lymph node	4, S5	(48, 49)
T1015A	LAU1015	Metastasis	visceral (lung)	4, S4B, S5	(48, 49)
T444C	LAU444	Metastasis	lymph node	4, S5	(106)
T1013A	LAU1013	Metastasis	lymph node	4, S5	-
Me235	LAU63	Metastasis	lymph node	S4B	(49, 96, 97, 103)
Me252	LAU119	Metastasis	lymph node	S4B	(49, 99)
Me260.LN	LAU149	Metastasis	lymph node	S4B	(49, 103, 107)
T1194B	LAU1194	Metastasis	lymph node	S4B	(49)
T1349A	LAU1349	Metastasis	lymph node	S4B	(49)
Me257	LAU145	Metastasis	skin	S4B	(49, 99, 108)
T311B	LAU311	Metastasis	lymph node	S4B	(49)
T333A	LAU333	Metastasis	skin	S4B	(49, 103)
T618A	LAU618	Metastasis	skin	S4B	(49, 96, 97, 102, 103, 109)
T975A	LAU975	Metastasis	brain	S4B	(49)
Me215	LAU48	Metastasis	lymph node	S4B	(49, 103)
T1257A	LAU1257	Primary tumor	rectal	S4B	(49, 103)
T362C	LAU362	Metastasis	skin	S4B	(49)
T640A	LAU640	Metastasis	skin	S4B	(49)
T685A	LAU685	Metastasis	skin	S4B	(49)

Refs. indicate published work describing the cell lines.

Table S4. A selection of currently active clinical trials of CSF1 or CSF1R blockade in combination with immune checkpoint blockade (ClinicalTrials.gov; 18 October 2017).

Compound/Class/Target	Clinical phase	Sponsor	Tumor type	Reference
PLX3397/TKI/CSF1R and Durvalumab/mAB/PDL1	I	Plexxikon Astra Zeneca	Metastatic/advanced colorectal or pancreatic cancer	NCT02777710
PLX3397/TKI/CSF1R and Pembrolizumab/mAB/PD1	I/IIa	Plexxikon	Melanoma, NSCLC, SCC of head & neck, GIST	NCT02452424
ARR-382/TKI/CSF1R and Pembrolizumab/mAB/PD1	I/II	Array BioPharma	Advanced solid tumors	NCT02880371
BLZ945/TKI/CSF1R and PDR001/mAB/PD1	I/II	Novartis Pharmaceuticals	Advanced solid tumors	NCT02829723
RG7155 (RO5509554)/ mAB/CSF-1R and MPDL3280A/mAB/PDL1	I	Hoffman-La Roche	Solid cancers	NCT02323191
FPA008/mAB/CSF1R and Nivolumab/mAB/PD1	Ia/Ib	Five Prime Therapeutics, Inc.	Advanced solid tumors	NCT02526017
AMG820/mAB/CSF1R and Pembrolizumab/mAB/PD1	I/II	Amgen	NSCLC, pancreatic and colorectal cancer	NCT02713529
LY3022855/mAB/CSF1R and Durvalumab/mAB/PDL1 or Tremelimumab/mAB/CTLA4	Ia/Ib	Eli Lilly	Solid tumor	NCT02718911
MCS110/mAB/CSF1 and PDR001/mAB/PD1	I/II	Novartis	TNBC, Melanoma, pancreatic and endometrial carcinoma	NCT02807844

NSCLC, non-small cell lung carcinoma; SCC, squamous cell carcinoma; GIST, gastrointestinal stromal tumors; TNBC, triple-negative breast cancer; TKI, Tyrosine kinase inhibitor; mAB, monoclonal antibody